Optics and Fluid Dynamics Department annual progress report for 1993

Hanson, Steen Grüner; Lading, Lars; Michelsen, Poul; Skaarup, Bitten

Publication date:
1994

Document Version
Publisher's PDF, also known as Version of record

RISØ

Risø-R-715(EN)

Optics and Fluid Dynamics Department Annual Progress Report for 1993

Edited by S.G. Hanson, L. Lading, P. Michelsen, and B. Skaarup

Risø National Laboratory, Roskilde, Denmark
January 1994

Optics and Fluid Dynamics Department Annual Progress Report for 1993

Risø-R-715(EN)

Edited by S.G. Hanson, L. Lading, P. Michelsen, and B. Skaarup

Risø National Laboratory, Roskilde, Denmark
January 1994

Abstract Research in the Optics and Fluid Dynamics Department is performed within the following two programme areas: optics and continuum physics. In optics the activities are within (a) optical materials, (b) quasi-elastic light scattering and diagnostics in solids, fluids, and plasmas, and (c) optical and electronic information processing. Within continuum physics the activities are within (a) studies of nonlinear c namical processes in continuum systems, (b) investigations of problems with relevance to fusion plasma physics. The injection of pellets in fusion experiments has been investigated and pellet injectors to European fusion experiments are manufactured. The department is also responsible for the EURATOM collaboration within fusion plasma physics. A summary of activities in 1993 is presented.

ISBN 87-550-1937-4
ISSN 0106-2840
ISSN 0906-1797

Grafisk Service, Risø, 1994

Contents

1 Introduction *5*

2 Optics *6*
- 2.1 Introduction *6*
- 2.2 Optical Materials *6*
  - 2.2.1 Optical Storage Properties of Side Chain Liquid Crystalline Polyesters *6*
  - 2.2.2 Bacteriorhodopsin - a Holographic Recording Material Derived from Bacteria *7*
  - 2.2.3 Photorefractive Subharmonics *8*
  - 2.2.4 Photorefractive Interference Filters *9*
  - 2.2.5 Photorefractive Interactions in the Presence of a Magnetic Field *11*
  - 2.2.6 Fundamental Laser Ablation of Simple Materials *12*
  - 2.2.7 Applications of Intense UV-Laser Irradiation and Ablation of Solids *13*
- 2.3 Diagnostics *14*
  - 2.3.1 Speckle Statistics and Interferometric Decorrelation effects *14*
  - 2.3.2 Speckle Noise in Laser Velocimetry *16*
  - 2.3.3 Optical Measurements of Ocean Waves *17*
  - 2.3.4 Polarisation Dependency of Radar Backscattering from the Ocean Surface *18*
- 2.4 Information Processing *19*
  - 2.4.1 A Q-State Mean Field Annealing Algorithm for Filtering of Grey Level Images Suited for Optoelectronic Implementation *19*
  - 2.4.2 Nonlinear Noise Filtering and Texture Recognition by an Optoelectronic Neural Network that Implements a Mean Field Annealing Algorithm *22*
  - 2.4.3 Optical Processing in Industrial Applications *23*
  - 2.4.4 Machine Stereo Vision *25*
  - 2.4.5 Automatic Pig Evisceration - 3D Image Analysis *26*
  - 2.4.6 Neural Network Hardware for Image Processing *27*

3 Continuum Physics *27*
- 3.1 Introduction *27*
- 3.2 Nonlinear Dynamics of Continuum Systems *28*
  - 3.2.1 Simulation of Viscoelastic Fluids *28*
  - 3.2.2 Studies of Boundary Layer Formation and Detachment in Two-Dimensional Flows *28*
  - 3.2.3 Development of Accurate and Efficient Numerical Algorithms for the Solution of Problems with Sharp Variations *30*
  - 3.2.4 Numerical and Analytical Studies of Transitions in Circular Shear Layers *31*
  - 3.2.5 Multidomain Spectral Simulation of Unsteady, Compressible Flow Around a Circular Cylinder *33*
  - 3.2.6 Linear Stability of a Modon on the β-Plane *34*
  - 3.2.7 Dipole Formation from Breaking Rossby Waves *35*

3.2.8 Dynamics of Nonlinear Dipole Vortices *35*
3.2.9 Interaction of Dipolar Vortices with Cylinders *37*
3.2.10 Experimental Studies of Dipole Interaction with Walls in 2D Flows *39*
3.3 Fusion Plasma Physics *39*
3.3.1 Experimental Investigations of Two-Dimensional Plasma Turbulence *39*
3.3.2 Experimental Evidence for Mode Selection in Turbulent Plasma Transport *41*
3.3.3 Modulational Instability of Plasma Waves in Two Dimensions *42*
3.3.4 Plasma Transport Due to Electrostatic Turbulence *44*
3.3.5 Visualisation of Numerical Data *44*
3.3.6 A Phase Screen Approach to Coherent Scattering in Fluids *45*
3.3.7 Experimental Investigation of Edge Localised Modes in JET *45*
3.3.8 Magnetic Stresses in Ideal MHD Plasmas *46*

4 Pellet Injectors for Fusion Experiments *47*
4.1 Introduction *47*
4.1.1 Construction of Multishot Pellet Injectors for FTU, Frascati, and RFX, Padova *48*

5 Publications and Educational Activities *49*
5.1 Optics *49*
5.1.1 Publications *49*
5.1.2 Unpublished Contributions *51*
5.2 Continuum Physics *53*
5.2.1 Publications *53*
5.2.2 Unpublished Contributions *54*

6 Personnel *56*

1 Introduction

The department performs basic and applied research within continuum physics and optics. The scope is both understanding of physical phenomena and development of materials and systems for specific applications. The activities are often performed in collaboration with other research groups and industry. The training of students at a graduate level is an integral part of the activities and so is the dissemination of the results to research and industry. The results are important for the understanding of the dynamics of fluids including fusion plasmas, as well as for the understanding of optical diagnostic systems and new optical materials. Several of the results are exploited by industry.

The motivation for the combination of optics, fluid dynamics, and plasma physics is that most of the activities lie within what can be called continuum physics. Several of the basic theoretical tools are similar. In addition to this fact most of the optical work on diagnostics/measurement science is concentrated on fluid applications.

The work described in this report falls within the following categories:

- *Continuum physics* is concentrated on basic physical phenomena with relevance to fusion in plasmas as well as to other fluid dynamic systems. Coherent structures, turbulent transport, and general nonlinear phenomena are investigated. Both theoretical, numerical, and experimental work is performed. A significant effort is devoted to the development of efficient reliable spectral models investigated on computers. Experimental work is performed in turbulent plasmas and in shallow rotating water flows.

- *Pellet injection* systems have been developed and are now delivered to other fusion research laboratories. Work is also performed on the pellet plasma interaction.

- *Optical materials and light propagation* are concentrated on nonlinear phenomena, storage materials, and propagation in random media.

- *Diagnostic methods* for probing the state of both fluid mechanical systems and systems based on solids are investigated.

- *Optical and electronic information processing* incorporates work on two-dimensional optical transforms applied to pattern recognition. Schemes for pattern recognition for inspection and control are being developed.

Of major results in 1993 can be mentioned:

- A novel image processing scheme for processing of flexible objects (food) was developed and is being implemented in connection with an EU-BRITE project. A very fast neural network processing board was developed for the application.

- A novel nonlinear opto-electronic method for texture recognition was developed.

- The generation of spatial and temporal subharmonics in photorefractive crystals was verified and modelled.

- Phenomena related to speckle statistics with applications to dynamic measurements within a very broad range of the electromagnetic spectrum were discovered.

- A pellet injector for plasma fusion research was delivered to ENEA, Italy.

- Three companies associated with the department were established in the Center for Advanced Technology.
- The experimental plasma investigations on the turbulence and transport in the Q-machine for plasma physics research were completed and the Q-machine was dismantled.

2 Optics

2.1 Introduction

Three major themes form the basis for the work in the Optics Section, each of which is nourished by the outcome of the others. In this way the diversity of the work field provides relations, bringing about new tools to related areas.

- *Optical materials*
  The work in this field serves as a common basis from which knowledge about new relevant materials emanates. Many interesting applications in optical processing await the arrival of optical films with dedicated properties. Industrial use of parallel processing, as it is inherent in optical processing, calls for fast, nonlinear response in commercially available optical elements. The study of such materials is conducted with a large effort in the section and the progress is scrutinised for future use in optical processing and in future optical sensor systems.
- *Diagnostics*
  The work in this field comprises industrial sensor development as well as theoretical work on optimising general optical measuring systems. With the arrival of low-cost optical sources and array detectors, new optical systems become of relevance to a broader range of the industrial market. Combined with holographic optical elements, these building blocks open new areas in mechanical measurements as well as for medical applications.
- *Information processing*
  Information processing is pursued along two different directions. Electronic processing of images is carried out by setting up a neural network algorithm that has now been optimised by designing a PC-card dedicated to this task. Several projects will benefit from the rate at which pattern recognition and quality control can be conducted. A combination of electronic and optical processing has been implemented. The inherent speed of the optical part of the system is employed in a closed optical loop, whereas the computational power of the electronic processor is devoted to updating electronically addressable optical filters.

2.2 Optical Materials

2.2.1 Optical Storage Properties of Side Chain Liquid Crystalline Polyesters

(P.S. Ramanujam, S. Hvilsted (Solid State Physics Department), and F. Andruzzi (CNR, University of Pisa, Italy))

Several side chain liquid crystalline (SCLC) polymer systems containing pendant azo dyes exhibit permanent local polymer main chain conformational reorganisation in response to light due to trans-cis isomerisation resulting in local changes

in the refractive index. This system presents a flexible architecture with several adjustable design parameters, such as the length of methylene sequence in the polyester main chain, the length of the flexible methylene spacers in the side chain, and the molar mass of the polyester. Each parameter has been demonstrated to affect the behaviour of the thin polyester films under irradiation by light from an argon ion laser. We have investigated the implications due to a change in the length of the flexible spacer and that of the acidic constituent of the main chain for optical storage through measurements of the optical anisotropy. The side chains discussed here contain 6, 8, and 10 methylene spacers and the main chain contains 3 to 14 methylene groups.

The films have been produced by dissolving 2 mg of the polyester in 200 microlitres of chloroform and gravity settling on a glass substrate. The films are not preoriented. The time dependent measurements of the optically induced anisotropy were performed with the polyester films between crossed linear polarisers. A HeNe laser was used to measure the transmission through the films. A polarised argon ion laser beam at 488 nm with its polarisation at 45 degrees to the linear polariser orientation was used to induce the optical anisotropy in the film. It is shown that the transmission through the films depends on the laser intensity, and that the polyesters with shorter flexible spacers respond more readily to low irradiation intensities albeit with longer time constants. The time constants are typically between 10 and 100 s. The maximum transmission for these films lies between 60% and 85% of the incident red light for irradiation times larger than 200 s. Polyesters with short flexible spacers display only a small decay of the transmitted light after the argon laser has been switched off. We have found that in certain cases, especially when the main chain contains 4 to 8 methylene spacers, the red laser is capable of orienting the molecules even after switching off the writing laser. The red laser aligns the azobenzene moieties parallel to its polarisation. These results have been confirmed through polarised Fourier transform infrared spectroscopic measurements. This points to hitherto unreported photophysics induced by red light in azobenzene moieties.

2.2.2 Bacteriorhodopsin - a Holographic Recording Material Derived from Bacteria

(L.R. Lindvold, H. Imam, and P.S. Ramanujam)

Throughout the past 20 years a vast amount of effort has been devoted to holographic memories to demonstrate the scalability, compactness, and integratibility of parallel optical technologies. One of the objectives necessary in order to meet this aim is to implement a reconfigurable holographic memory. This is the topic of a current research project, POPAM, supported by the European Union under the Basic Research Programme. The material that has been chosen to function as erasable storage material is bacteriorhodopsin.

Bacteriorhodopsin is a naturally occurring photochromic protein present in the so-called purple membrane that partly constitutes the cell membrane in certain halophilic bacteria. The photochromic cycle of the purple membrane is quite unique; the ground state has a broad absorption band with a peak centred at 570 nm (light adapted bacteriorhodopsin), and a metastable state centred at 413 nm with a thermal relaxation time of 10 ms. The metastable state offers two potential advantages. First, it can be stimulated by either electrical fields or photons to decay into the ground state in 200 ns. Secondly, the thermal relaxation time of this state can be extended by 5 orders of a magnitude by suitable chemical treatment of the purple membrane, without compromising the stimulated decay of 200 ns.

The work has so far been aimed at establishing the sufficient handling procedures as well as film fabrication techniques for this material. Although the diffraction efficiency, 0.5%, is modest compared with other real-time holographic recording materials, it exhibits high sensitivity (10 mW/cm^2 @ 454 nm) with a response time of a few ms. Furthermore, the material can be recycled more than 100 times without fatigue. Experiments carried out so far have shown a flat spatial frequency response up to 2500 lines/mm. Through chemical modifications of the film forming matrix, gelatin, the lifetime of the M-state has been extended from 10 ms to 5 min.

The bacteriorhodopsin films have also proved to possess highly nonlinear properties. Both formation of dark solitons and photoinduced anisotropy have been demonstrated with a HeNe laser (= 632.8 nm) at few milliwatts of power.

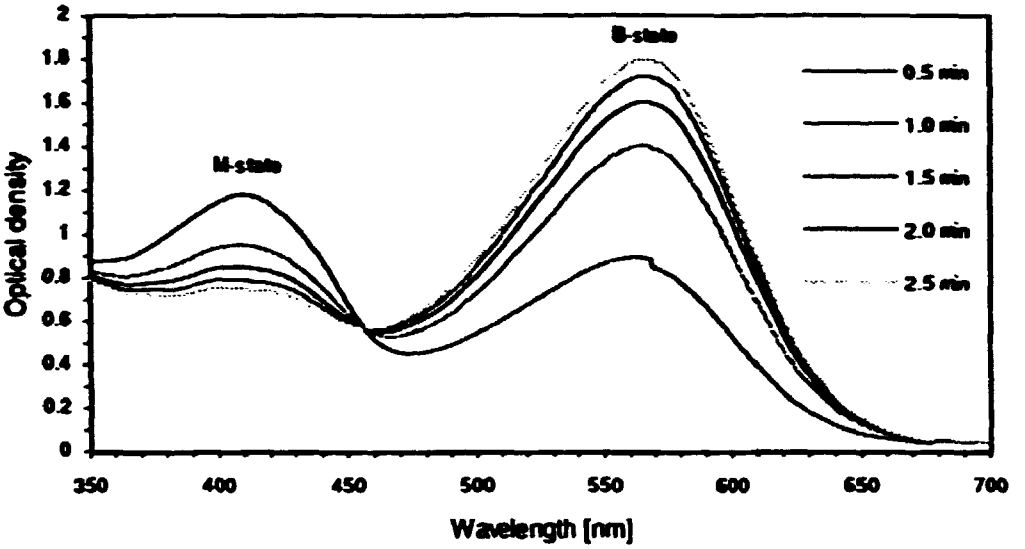

Figure 1. Spectroscopic recording of the thermal decay from M- to B-state. The bacteriorhodopsin was immobilised in a gelatin film with a thickness of 75 microns and a pH = 9. The bR film was photoexcited by flooding the sample in the spectrophotometer with a spotlight for 1 min. just before starting the time-lapsed scans.

2.2.3 Photorefractive Subharmonics

(H.C. Pedersen and P.M. Johansen)

The generation of subharmonics in photorefractive media is a new and interesting phenomenon. New basic knowledge about photorefractive effects emerges. In dealing with photorefractive interaction it is common to assume that the induced space-charge electric field grating reflects the period of the optical intensity distribution incident to the crystal. Recently, however, it was shown that under certain experimental conditions spatial subharmonics of the fundamental spatial frequency, i.e. gratings with spatial period K/n, where n is an integer, may be generated spontaneously in photorefractive media. In Fig. 1 the basic setup for generating subharmonics is shown. The generation of such gratings relies on the intrinsic nonlinearities of the equations governing the response of such materials to the incident optical fields. Furthermore, it has been shown that the fundamen-

tal space-charge field grating for certain regions of parameters becomes unstable against the subharmonic gratings. This effect can be seen from Figs. 1a and 1b. The purpose of the present project is to investigate the spontaneous generation of subharmonic beams due to the inherent nonlinearity of the photorefractive effect itself. It can be shown that only by illuminating with a moving interference pattern or by applying an AC electric field can the subharmonics be observed. The present project involves the basic study of such nonlinear processes including the stability conditions for the existence of subharmonics. The work is carried out in connection with the Continuum Physics Section in the department.

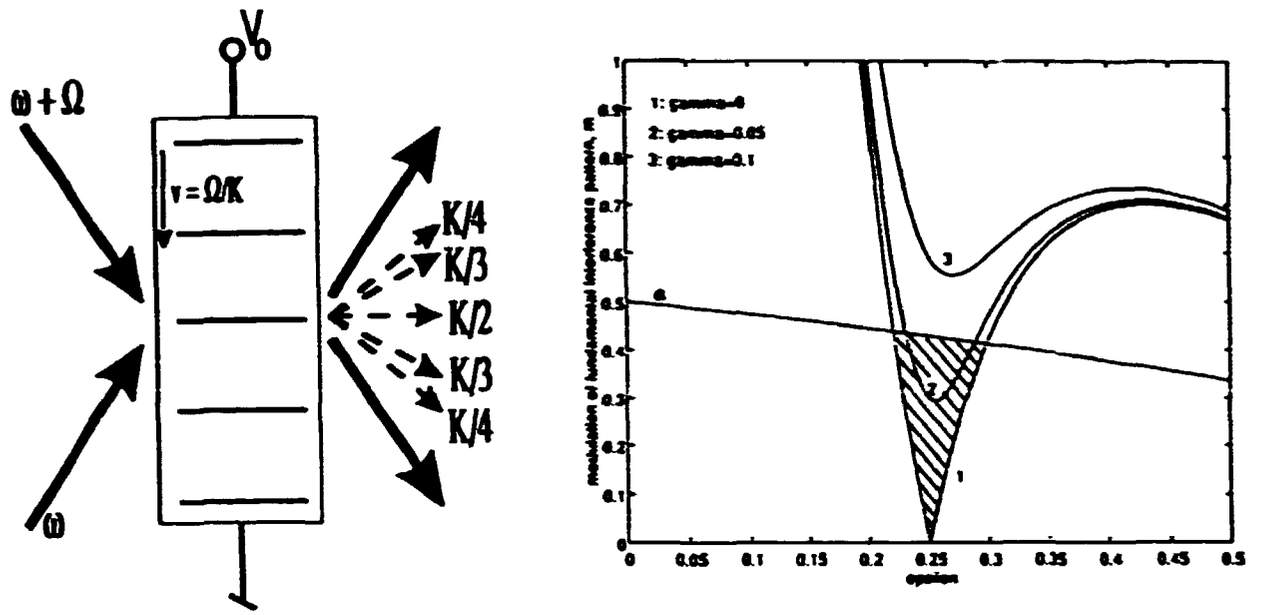

Figure 1a. Optical setup for subharmonic generation in photorefractive materials. Figure 1b. Regions of instability of the fundamental grating against the K/2 subharmonic.

2.2.4 Photorefractive Interference Filters

(C. Dam-Hansen, P.M. Johansen, and P.M. Petersen (The Technical University of Denmark))

Photorefractive materials have been used for many diverse applications among which the interference filters are a prominent member. Such filters generated in photorefractive crystals have very high wavelength selectivity as compared with ordinary dielectric mirrors, and offer several external control parameters. The filters are written by two coherent laser beams incident to the photorefractive crystal of $LiNbO_3$. The two laser fields induce a periodic change, with periodicity Λ, in the refractive index of the material. A third beam incident to the crystal face experiences varying layers of high and low indices of refraction. The situation experienced by this beam is analogous to that experienced in a multilayer dielectric mirror with alternating quarterwave layers of high and low indices of refraction. In the present situation, however, the layer thickness is *Lambda/2*. If the thickness is equal to a quarter of a wavelength for the laser field, the reflected wave from all

layers will interfere constructively at the front surface of the crystal and a strong reflected signal from the filter is obtained. The theory for conventional interference filters is extended to include the generic type of photorefractive filters[1]. It is shown that the reflectivity can be controlled externally by changing the angle between the two laser fields writing the periodic index variation, and by changing the relative strength of these beams (changing the optical modulation). It is shown that with such filters it is possible to obtain a reflectivity which approaches unity and, furthermore, the filter characteristics can be adjusted in real time. In the experiments performed here a close fit with theory is measured and a field of view of 6 mrad has been found which corresponds to a full-width-half-maximum bandwidth of 0.05 Å. Furthermore, such filters provide a method for probing the existence of higher spatial harmonics in the induced refractive index[2]. This work is a joint project between Risø and The Technical University of Denmark.

1) Dam-Hansen, C., Johansen, P.M., and Petersen, P.M. (1993). Dynamics of Photorefractive Interference Filters, submitted to JOSA B: Optical Physics, November 1993.

2) Petersen, P.M. and Johansen, P.M. (1993). Higher Spatial Harmonics in Nonlinear Photorefractive Interference Filters, presented at "The First International Symposium on Lasers and Optoelectronics Technology and Applications", held in Singapore, 11-14 November 1993.

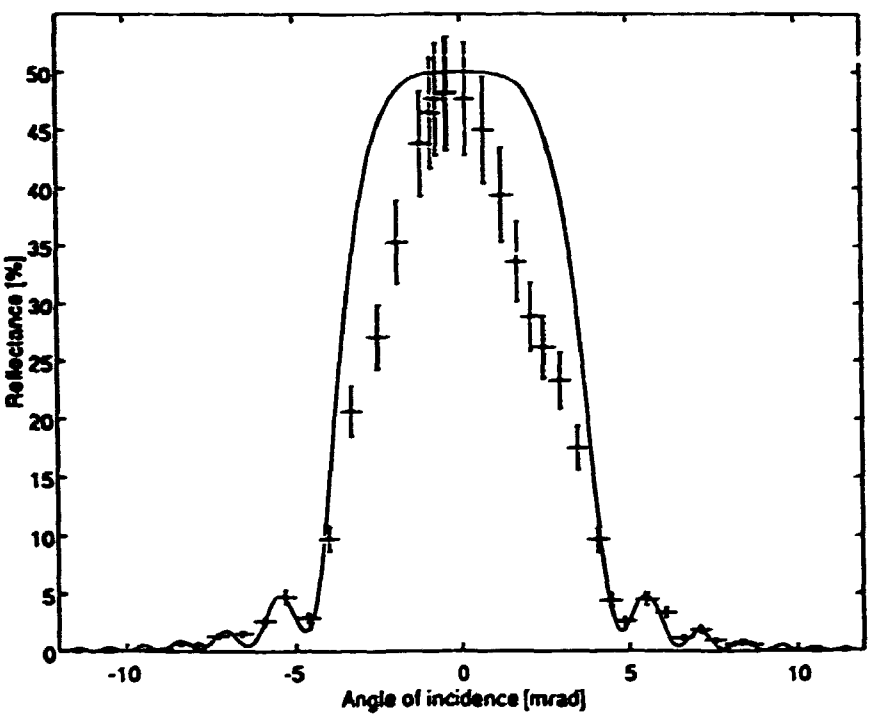

Figure 1. Comparison of measured (points with error bars) and theoretical (solid line) reflectance for a photorefractive filter written in a 2 cm long lithium niobate crystal versus the internal angle of incidence. The filter has a maximum reflectance of 48% and a field-of-view of approximately 6 mrad.

2.2.5 Photorefractive Interactions in the Presence of a Magnetic Field

(P.M. Johansen)

The existing formulation of two-beam coupling in photorefractive media has been extended to include the effects of an external magnetic field via the introduction of the Faraday effect which rotates the state of polarisation of the incident laser fields proportional to the magnitude of the magnetic field component along the direction of propagation of the fields. The effect of the magnetic field on the material refractive index is also taken into account. It is shown that the presence of such a magnetic field causes oscillations in the two-beam coupling strength of the material even in the case of materials with no optical activity. Furthermore, it is shown that the direction of the Faraday effect can be controlled by controlling the direction of the externally applied magnetic field and, hence, in very favourable situations cancel the effect of optical activity and thereby strengthen the optical coupling between the two beams interacting in the photorefractive material. The numerical results obtained based on the formulated theory agree well with the experimental results reported for diluted magnetic semiconductors of CdMnTe where oscillating two-beam coupling was found. Moreover, the energy coupling is found to be strongly dependent on the polarisation of the pump beam.

1) Johansen, P.M. Two-Wave Mixing with Externally Applied Magnetic Field and Faraday Effect in Photorefractive Media, to be published in IEEE J. Quant. Electron.

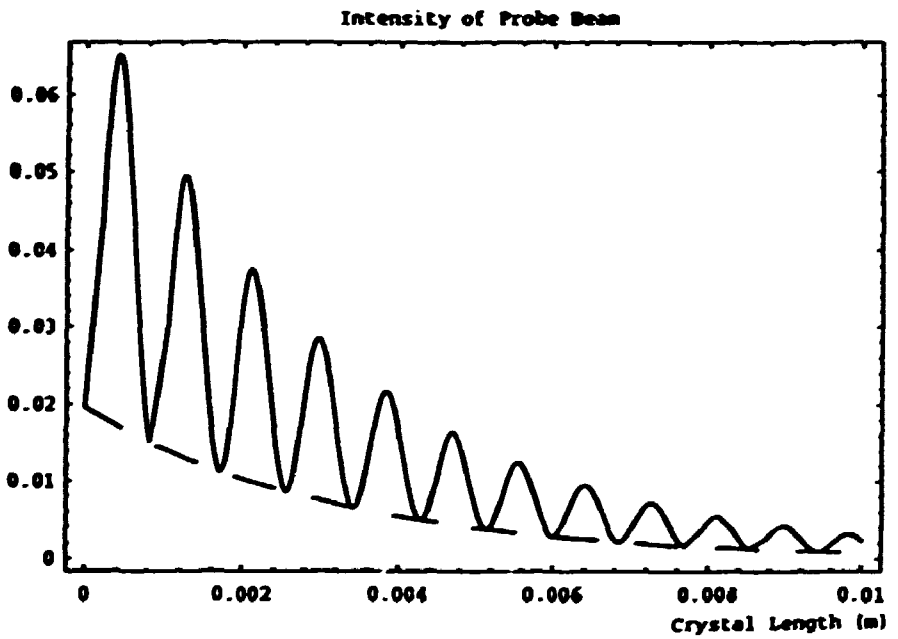

Figure 1. Intensity of the probe beam in CdMnTe as a function of the distance in the crystal for a 10 mm crystal. The applied electric field is $E_0 = 10^6$ V/m. The grating spacing is $\Lambda = 38$ μm, the applied frequency shift is $\Omega = 94$ rad/s. The angle between the z-axis and B_0 is $\delta = 45°$, and the angle between the grating wave vector and the applied electric field is $\Psi = 20°$. The dashed curve shows the situation with $B_0 = 0$ T whereas the solid line represents the $B_0 = 2$ T situation. The optical activity is zero so the oscillations are due only to the Faraday effect.

2.2.6 Fundamental Laser Ablation of Simple Materials

(J. Schou, W. Svendsen, A. Nordskov, and O. Ellegaard (University of Odense))

Laser ablation of solids, i.e. erosion by an intense laser beam, has gradually become one of the most important methods for depositing thin film and for investigating the mass composition of complicated organic mixtures. In particular, epitaxial films of high Tc-superconductors have been produced by UV-laser ablation deposition at many laboratories. Mass spectrometry of organic matrices doped with small amounts of bioorganic materials can be carried out in a fast and convenient manner by UV-laser irradiation.

However, the success of these methods does not mean that the basic processes are known. In most of the cases the studies have been performed in an empirical manner. In contrast to the main areas of physics, most of the materials investigated so far are fairly complex, whereas the simple ones have been studied to a relatively small extent.

The first step of an erosion of an insulator by laser ablation is the production of defects. The defects are typically strong absorbing centres so that the photon energy is efficiently converted to kinetic energy of the target molecules or heat. Obviously, the production rate of the laser-induced defects plays an important role for the ablation of insulators in the initial stage. In metals the photon energy is directly absorbed by the free electrons. In later stages an absorbing plume of ejected material develops in front of the target for insulators as well as metals.

These partly unexplored phenomena have stimulated a programme in which the basic processes of laser ablation from simple materials will be studied. The setup is shown in Fig. 1. The laser beam from a pulsed Nd:YAG laser strikes the target and produces a plume of material that leaves the target within a few nanoseconds. The ablated material will be collected on microbalances so that the

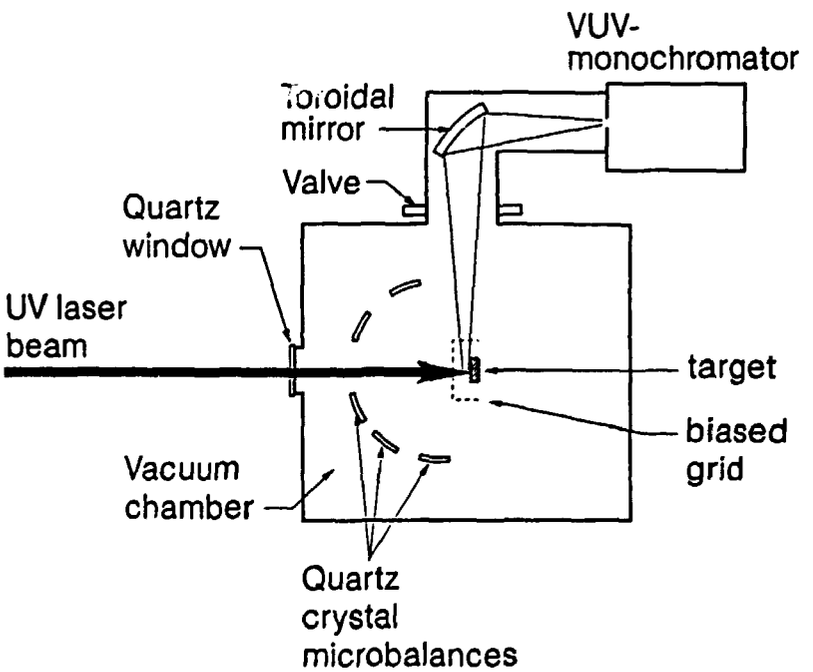

Figure 1. Schematic drawing of the setup for fundamental laser ablation.

erosion and deposition yield can be determined as a function of intensity and wavelength. Simultaneously with these measurements, the plume will be studied optically with a VUV-monochromator, and the emission of positive ions from the biased target will be estimated from the collected current.

Silver will be studied since there exist a few measurements of ablation from thin silver films and massive targets. Furthermore, silver surfaces develop comparatively little contaminants in vacuum. Water ice will be studied as well since this is one of the simplest oxides. Many of the electronic transitions are known for the water molecule. Water ice has recently been utilised as a matrix for sequences of DNA-dopants. With respect to the vacuum conditions, films of water ice are relatively easy to produce in situ and can, therefore, be kept comparatively clean.

2.2.7 Applications of Intense UV-Laser Irradiation and Ablation of Solids

(J. Schou, A. Nordskov, P.M. Johansen, P.S. Ramanujam, and L. Lindvold)

Laser irradiation of solids with intense UV-light leads to the production of defects as well as direct erosion by ablation. The precise excitation by monoenergetic photons can be utilised in many fields (Fig. 1). Even though the specific processes for the defect production and the ablation are relatively unexplored for many materials, the applications become increasingly important. The studies of fundamental laser ablation partly provide the basic programme necessary for successful achievement of the applications.

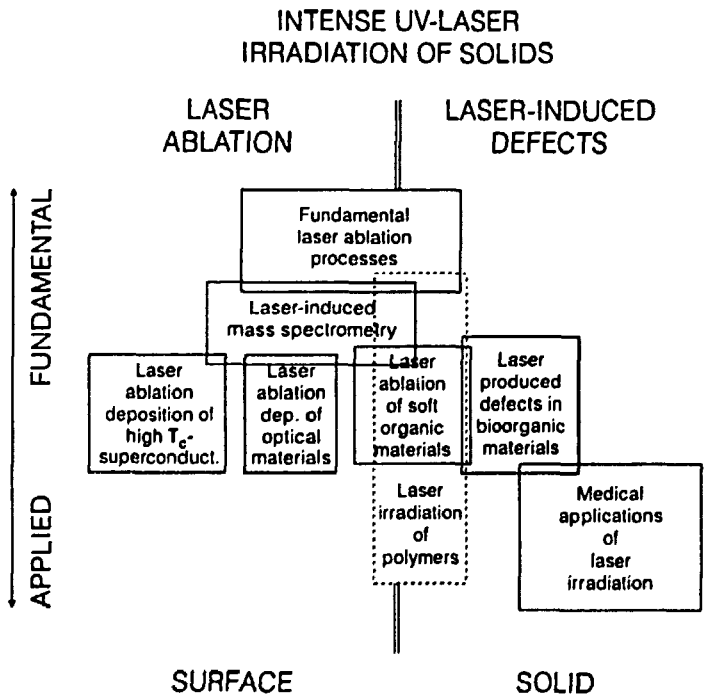

Figure 1. Schematic survey of possible applications of intense laser irradiation of solids.

A straightforward application of irradiation by a beam of monoenergetic photons is patterning of bacteriorhodopsin. A beam of sufficient intensity in the UV-regime may destroy the bonds selectively, whereas those in the areas covered by masks are intact. In the following steps it is possible to remove the material that contains these laser-produced effects with other methods. This procedure is well suited for patterning.

InSnOx has the particular property that it is a transparent electrical conductor. This material has apparently not yet been produced by laser ablation deposition.

Film deposition of photorefractive materials such as $BaTiO_3$ may be controlled in such a manner that films can be grown on an appropriate substrate. Then it is possible to study how the nonlinear effects on the refractive index change from a few monolayers up to continuum distances. This transition may be studied with two-wave mixing.

Another important issue is the influence of a strong magnetic field on the refractive index of GaAs. The coupling of the magnetic field to the index has been studied theoretically, but precise measurements have not been performed yet. The changes of the refractive index will be investigated with two-wave mixing from the Nd:YAG laser in a strong magnetic field at liquid helium temperature.

2.3 Diagnostics

2.3.1 Speckle Statistics and Interferometric Decorrelation effects

(S.G. Hanson, H.T. Yura (Electronics Technology Center, The Aerospace Corporation, USA), and B. Hurup Hansen)

Complex ray-matrix techniques combined with the paraxial approximation of the Huygen-Fresnel formulation of wave optics are a useful tool in the analysis of the performance of a rather general class of optical systems. This method expresses the complex optical field in the observation (or output) plane as an integral over an initial (or input) plane of a given source distribution multiplied by a propagation kernel. The propagation kernel is a function of the ABCD matrix elements of the complete optical system between the input and the output planes and properties of the intervening medium through which the light propagates. By using such methods it is possible to obtain in a straightforward manner expressions for all the statistical correlation functions that pertain to the optical system, the source distribution, and the intervening medium under consideration.

The use of complex ABCD matrix elements permits the modelling of limiting apertures (e.g., thin lenses, field stops, and finite-sized measurement apertures) as soft (i.e. Gaussian) apertures. In many applications such modelling yields useful engineering analytical approximations to system performance that can be used for designing, sizing, and scaling of optical systems.

We have considered the situation for homogeneous media[1]. Expressions for the following quantities have been obtained: the mean, the variance, and the corresponding correlation function of the irradiance distribution resulting from an incoherent source that has propagated through a complex, axially symmetric ABCD optical system. We have obtained general expression for the mutual coherence function, which can be regarded as a generalisation of the Van Cittert-Zernike theorem to complex paraxial ABCD systems. In the same manner expressions have been achieved for the number of speckles and the maximum number of independent intensity measurements permitted by the optical system. Analytical solutions to the problem of decorrelation in holographic interferometry and electronic speckle interferometry (ESPI) related to the fringe visibility have been obtained.

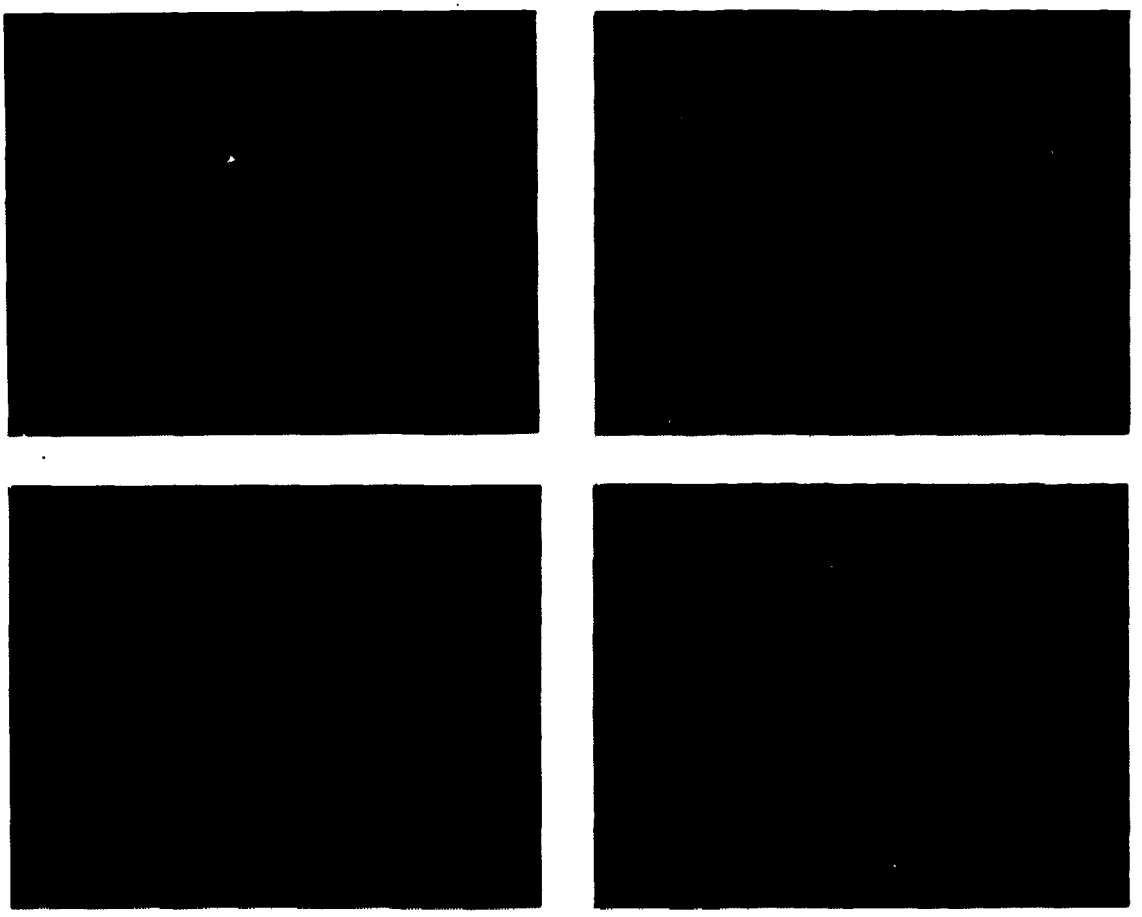

Figure 1. Various degrees of decorrelation observed in an electronic speckle interferometer from an object experiencing various degrees of in-plane tilt.

The decorrelations considered for the object are in-plane tilt, in-plane translation, and translation along the optical axis.

1) Yura, H.T., Hanson, S.G., and Grum, T.P. (1993). Speckle: statistics and interferometric decorrelation effects in complex ABCD optical systems, Journal of the Optical Society of America A 10, No. 2, February 1993, pp. 316-323.

2.3.2 Speckle Noise in Laser Velocimetry

(S.G. Hanson, L. Lading, H.T. Yura (Electronics Technology Center, The Aerospace Corporation, USA), and R.V. Edwards (Case Western Reserve University, Cleveland, Ohio, USA))

Two fundamental random processes appear to provide the fundamental limits to the uncertainty with which measurements can be performed: the photon shot noise process and the speckle process associated with the scattering. The speckle process modulates the photon process. It is from the detected modulation that the velocity is inferred.

We have considered the problem in connection with scattering from surfaces and especially in connection with the time-of-flight (two-spot) configuration. It

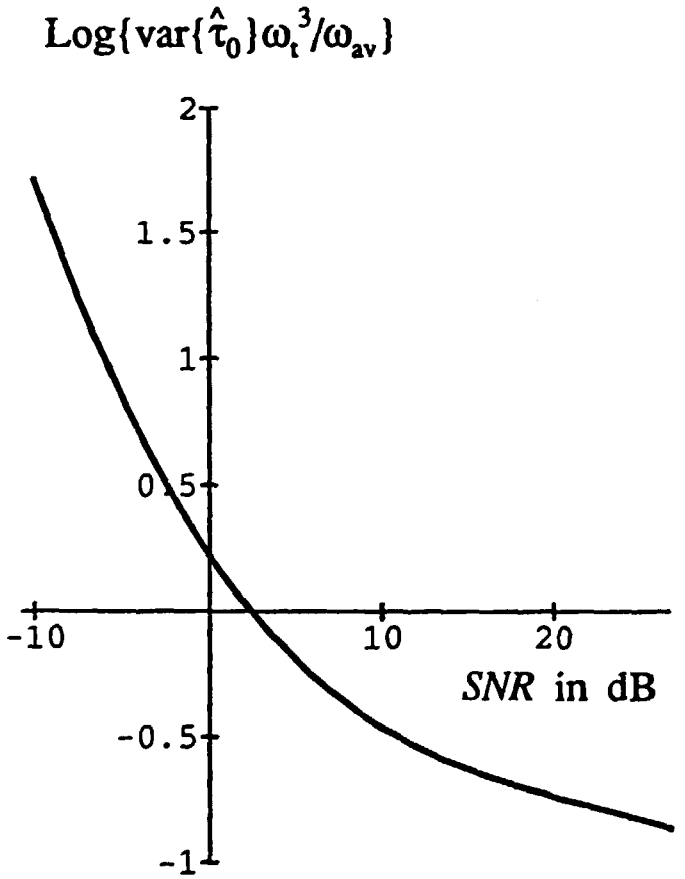

Figure 1. Minimum variance of the estimated time-of-flight versus the signal-to-noise ratio. The 'standard' limit in the case of no noise is one (log 1 = 0).

appears that the standard expressions for the statistical uncertainty, which may be obtained by considering the number of degrees of freedom over which the temporal averaging takes place, do not represent fundamental limits.

The effects of speckle decorrelation in connection with the absolute spatial bandwidth of the system set the lower limits to the measuring uncertainty. The speckle decorrelation has been analysed by the use of a complex ABCD matrix formulation[1]. In this analysis all apertures are assumed to be Gaussian. This appears to give legitimate results for speckle correlation effects. However, for the analysis of the actual measuring uncertainty, it appears that the limits are given by the fact that the transmitted and/or received beams are inevitably truncated by an aperture. Outside the aperture the light is blocked. Thus the spatial bandwidth is absolutely limited. It is this bandwidth that defines the ultimate lower limits to measuring uncertainty. A Gaussian beam would allow for arbitrarily high spatial frequencies - albeit attenuated but not eliminated.

If photon noise or thermal noise plays a significant role, the Gaussian beam analysis may still be valid[2].

1) Yura, H.T. and Hanson, S.G. (1993). Laser-time-of-flight velocimetry: analytical solution to the optical system based on ABCD matrices, Journal of the Optical Society of America A 10, No. 9, September 1993, pp. 1918-1924.

2) Lading, L. and Edwards, R.V. (1993). Laser velocimeters: lower limits to uncertainty, Appl. Opt. 32, pp. 3855-3866.

2.3.3 Optical Measurements of Ocean Waves

(S.G. Hanson, J. Churnside (Wave Propagation Laboratory, NOAA, Boulder, Colorado, USA))

An investigation of the possibility of optical measurements of ocean waves has been conducted in cooperation with Wave Propagation Laboratory, NOAA, Boulder, USA. Several techniques have previously been proposed for such measurements. The first one uses natural light reflected from the surface as a measure of the tilt of the surface. Stereophotography was later used to measure the height distribution of the surface, and lately a method has been introduced in which a laser beam penetrates the water-air interface from beneath. The beam position above the surface thus depicts the local slope.

Two new methods have been investigated. The first method is based on the delta-k lidar technique in which the backscattered light from one laser beam scattered from particles embedded in the water is analysed[1]. The laser beam consists of two different frequencies which set up a fringe pattern along the optical axis moving at the velocity of light as shown in Fig. 1. The fringe pattern is subsequently projected on the ocean surface, and resonance backscattering is observed from surface waves having a wavelength equal to half the period of the projection of the fringe pattern. The detected signal will be modulated with the difference frequency of the two laser beams and the wave velocity. This facilitates the probing of the phase velocity of a surface wave with known wave number. The calibration factors have been investigated with special emphasis on the linearity of the signal as a function of the wave height and as a function of the polarisation of the radiation. Further, the effect of measurement on waves riding on a large-scale swell wave has been addressed. When the swell intercepts the lidar beam at some other azimuthal angle, the situation is more complex and a horizontally or vertically polarised beam will no longer be perpendicular or parallel to the plane of refraction, and a mixed polarisation must be considered. Moreover, the effect of finite penetration depth of the light in water has been treated. As light penetrates water

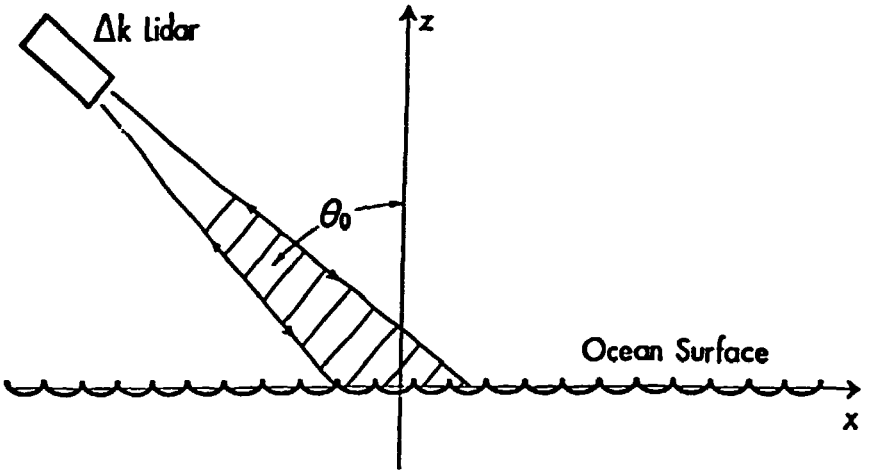

Figure 1. Geometry for a delta-k lidar system for measurements on the ocean surface.

and is scattered back to the surface, the projected fringe pattern may have moved thus creating echoes back to the detector, echoes which are out of phase with the signal coming from just beneath the surface. It is consequently important that the fringe period exceeds the penetration depth of the radiation. Finally, the wave number sensitivity and the angular sensitivity of the system have been considered.

A second method of interest is based on backscattering of incoherent light from particles suspended in water[2]. The ratio of backscattered intensity from two orthogonal polarisations will solely depend on the angle of incidence of the light and will be independent of the intensity and the amount of scattering particles as long as the particles are randomly oriented. Two images recorded with a CCD-camera will provide the necessary information for determination of the angle of incidence pixel by pixel. The spatial distribution of surface tilt can therefore be deduced from the imagery. The method has been verified in laboratory measurements.

1) Churnside, J.H. and Hanson, S.G. Effect of penetration depth and swell-generated tilt on delta-k lidar performance, accepted for publication in Applied Optics primo 1994.

2) Churnside, J.H., Hanson, S.G., and Wilson, J.J. Determination of ocean wave spectra from images of backscattered incoherent light, submitted to Applied Optics.

2.3.4 Polarisation Dependency of Radar Backscattering from the Ocean Surface

(S.G. Hanson and V.U. Zavarotny (Wave Propagation Laboratory, NOAA, Boulder, Colorado, USA))

The influence of forwardly reflected radiation from gravity waves on the backscattered radiation from a sea surface has been analysed[1]. Special emphasis has been given to the observed difference between imagery obtained for equal polarisation for the transmitter and receiver, i.e. horizontal and vertical. The basic scattering mechanism for the radiation is assumed to be Bragg scattering from matching capillary waves riding on trochoidally shaped gravity waves as shown in Fig. 1. For large angles of incidence, the back of the gravity wave will primarily act as

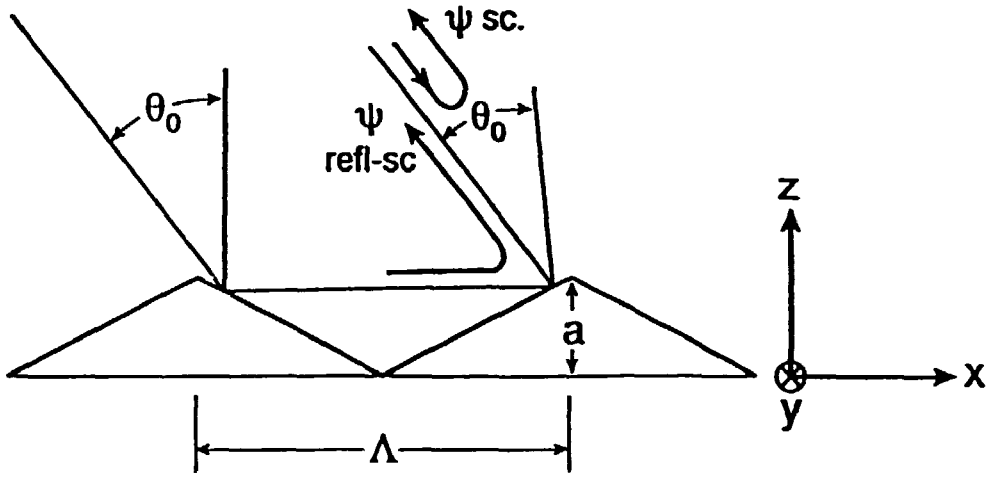

Figure 1. Scattering geometry for a triangular wave model. The plane of incidence is y = 0, and the angle of incidence is θ_0. Polarisation in the plane of incidence is denoted V-polarisation, while perpendicularly polarised radiation is denoted H-polarisation.

a reflector causing the radiation on the forward slope of the wave to consist of a coherent superposition of the directly incident wave and the reflected wave.

It has therefore been argued that probing of the spatial change of the shape of the gravity waves can be deduced from the backscattered intensity of microwaves of far lower wavelengths. Imagery obtained with horizontally polarised radiation will especially reveal these features. The multipath backscattering is identical to "enhanced backscattering" as it is known in the optical regime. This formalism will contribute to the explanation of "sea spikes" well-known in radar scattering from the sea surface and specially observed for horizontally polarised radiation.

The theory has shown that multipath backscattering may account for larger backscattering cross sections than the cross section from Bragg scattering itself.

1) Hanson, S.G. and Zavorotny, V.U. Polarization dependency of enhanced multipath radar backscattering from the ocean surface, submitted to IEEE Transactions on Antennas and Propagation.

2.4 Information Processing

2.4.1 A Q-State Mean Field Annealing Algorithm for Filtering of Grey Level Images Suited for Optoelectronic Implementation

(J. Glückstad and T.M. Jørgensen)

Algorithms for extraction of features within noise are important as a preprocessing stage for automatic image recognition. It is important that such algorithms are fast and parallel schemes are therefore preferable. The so-called mean field annealing algorithms have proved to be preferable to simulated annealing algorithms since less iteration steps are needed. We have considered a mean field annealing algorithm that corresponds to a Q-state spin-Ising model. The algorithm is used for nonlinear noise filtering of images into Q grey levels. Each iteration of the specific scheme involves a bias field addition, a convolution operation, and a nonlinear operation corresponding to a multilevel threshold operation (see Fig. 1).

Software implementations of the algorithm have produced convincing results,

even for signal-to-noise ratios well below one (see Fig. 2).

Since the convolution operation corresponds to an averaging procedure over neighbouring pixels, it can be performed in parallel by the use of a defocusing camera. We have implemented the scheme by the use of a spatial light modulator, a camera, and a frame grabber. The image is displayed on the light modulator and the nonlinear operations are performed by the use of the frame grabber. Due to inhomogeneities in the illumination of the light modulator the operational number of levels of the threshold curve is limited. However, our results act as a proof of principle with respect to an optoelectronic parallel implementation (see Fig. 3).

The low-pass filter used in the loop can be considered to be an example of a simple wavelet filter which determines the features we are looking for in the noisy image. By changing the size of the filter the scale of the specified structures changes. A possible application of such filters would be in the area of defect detection.

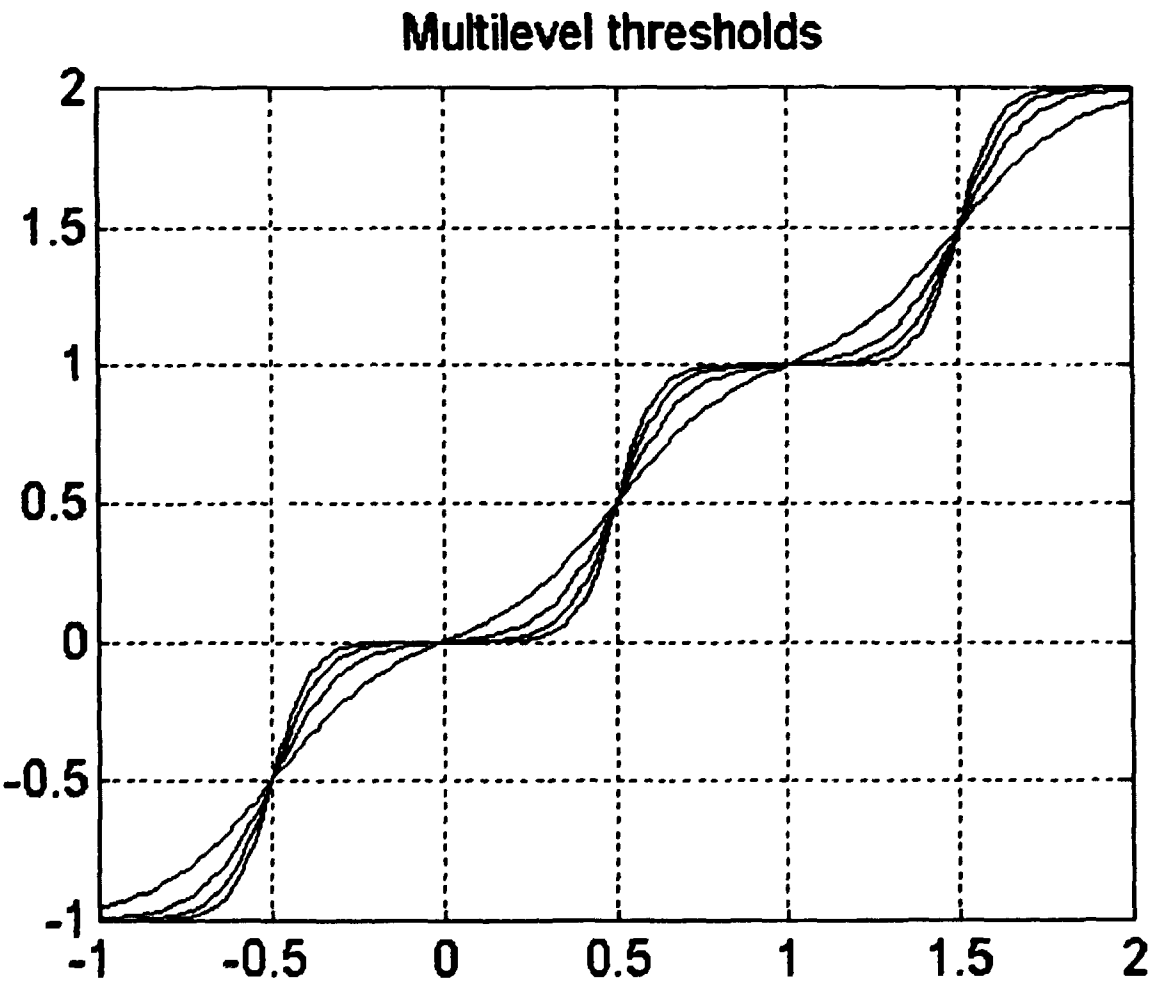

Figure 1. The multilevel thresholding functions used in the loop. The steepness is increased during the iterations corresponding to the annealing scheme.

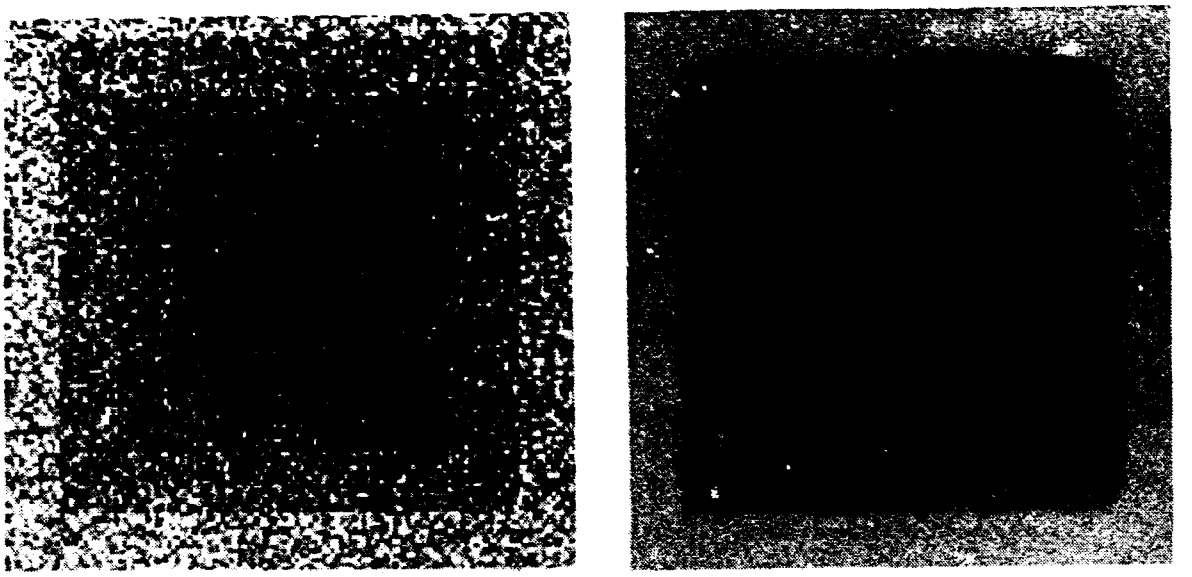

Figure 2a. Noisy image. Figure 2b. Resulting image after eight iterations (computer simulation).

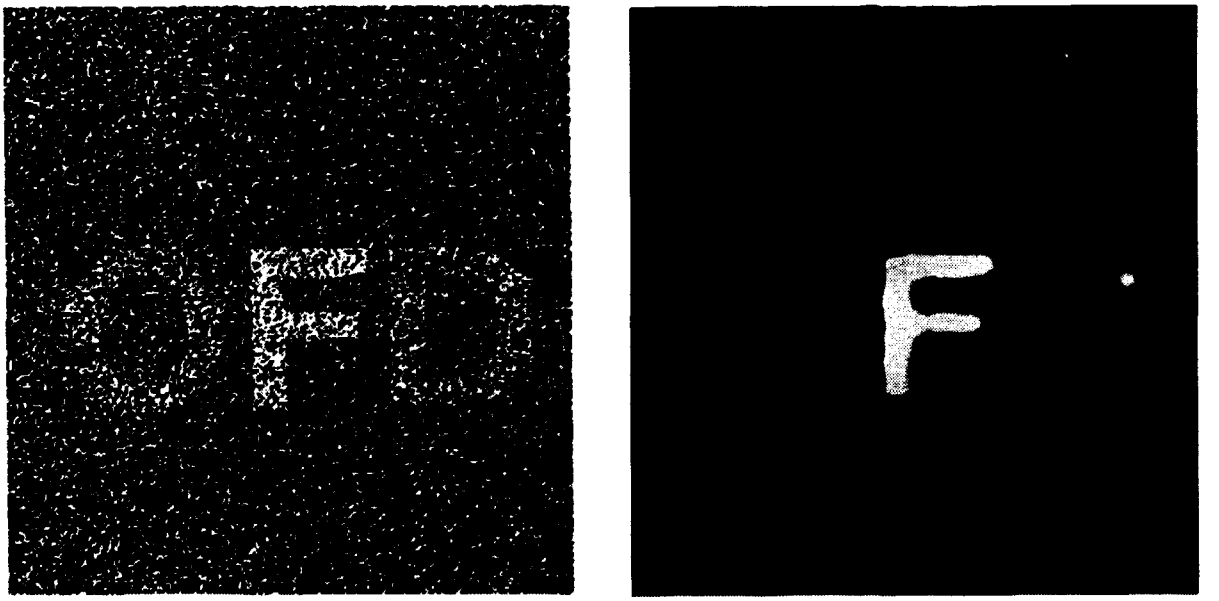

Figure 3a. Noisy image. The standard deviation of the Gaussian noise corresponds to 1.5 times the step size between two neighbouring grey levels of the underlying image. Figure 3b. Resulting image after four iterations through the optoelectronic loop.

2.4.2 Nonlinear Noise Filtering and Texture Recognition by an Optoelectronic Neural Network that Implements a Mean Field Annealing Algorithm

(T.M. Jørgensen and J. Glückstad)

Instead of extracting coherent pixel clusters, structures from noisy images as described in the above section may be obtained by considering the more general task of texture recognition. Texture analysis is of importance in many areas. Some of the most common applications are: classification of aerial images, medical image

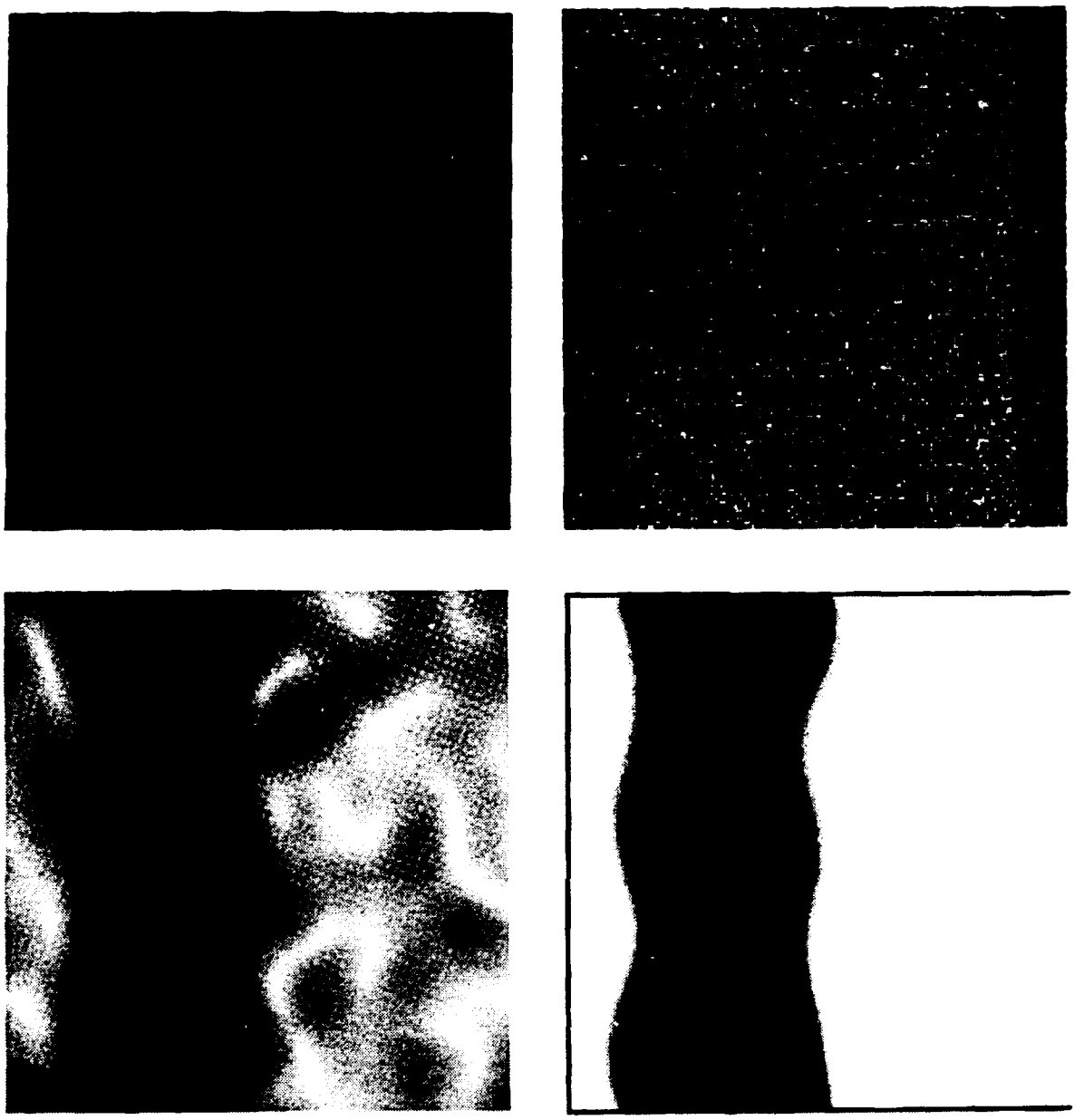

Figure 1a. Two test textures. Figure 1b. Test textures with added Gaussian noise. Figure 1c. Local energy map corresponding to one of the two textures. Figure 1d. Resulting image after eight iterations with image 1c as input (computer simulation).

processing, and process control.

In order to deal with textures we make use of the fact that most textures can be characterised by their energy distribution in a set of windows of the spatial frequency space. The concept is therefore to make use of the so-called local energy maps of specific spatial frequency regions. These energy maps can be considered to be the result of filtering the textures with quadratic Gabor-like filters, and squaring and summing the resulting quadrature filter outputs. Optically the local energy map can simply be obtained by situating a simple bandpass filter in the Fourier plane of the setup. An appropriate combination of these energy maps is then used as input to a loop similar to the one presented above. To illustrate this concept consider the two textures (from Brodatz album) in Fig. 1a. Adding Gaussian noise with a standard deviation equal to the modulation depth of the texture signal we obtain the image shown in Fig. 1b. Using a bandpass filter around the basic frequency of the left texture the local energy map becomes as shown in Fig. 1c (computer simulation). The local energy map is then processed by a loop which basically corresponds to the one described above. The resulting image after eight iterations is shown in Fig. 1d (computer simulation). It is seen that the algorithm determines the region of interest quite well in spite of the noise. We have also tried to use multiplicative noise and combinations of additive and multiplicative noise. Using signal-to-noise ratios of the size corresponding to that of Fig. 1b the results for these cases become similar to the one given by Fig. 1d.

This work was supported by the National Research Councils under the CONNECT programme.

2.4.3 Optical Processing in Industrial Applications

(A. Skov Jensen, E. Rasmussen, B. Hurup Hansen, and E. Eilertsen)

The ESPRIT project, NAOPIA II, was started in January 1993 with partners from Thomson-CSF, PSA, IOTA (France), University of Erlangen, DASA, JenOptik (Germany), Alenia (Italy), and Risø. The objective of the project is to demonstrate an industrial application utilising optical technology for the industrial partners in the project (PSA, DASA, Alenia, and JenOptik).

Risø is responsible for the following two tasks:

- To build an XY-traversing work cell with camera and computer controller interface for the purpose of making a demonstrator for the assembly of composite materials (airplane parts). An operator is supposed to lay plies of composite materials in a prescribed order to build the wanted part. The camera-computer system must check whether the operation has been performed correctly. Originally it was planned that the control should be done with an optical joint transform correlator, but experiments and simulations have shown that this is not feasible. The application of optics in this task is limited and consists mainly of the illumination system produced by University of Erlangen. The work cell is shown in Fig. 1.
- To produce a double, electrically addressed, active matrix spatial light modulator (SLM) with the assistance from a subcontractor from Minsk Radioengineering Institute (MRI), Republic of Belarus. The SLM is supposed to be used as an input SLM to the optical joint transform correlator built by Thomson-CSF. The specifications of the SLM are:
  - The SLM is a double 480*480 pixel device with a distance of 3 mm.
  - The speed of the SLM is TV-frame rate.

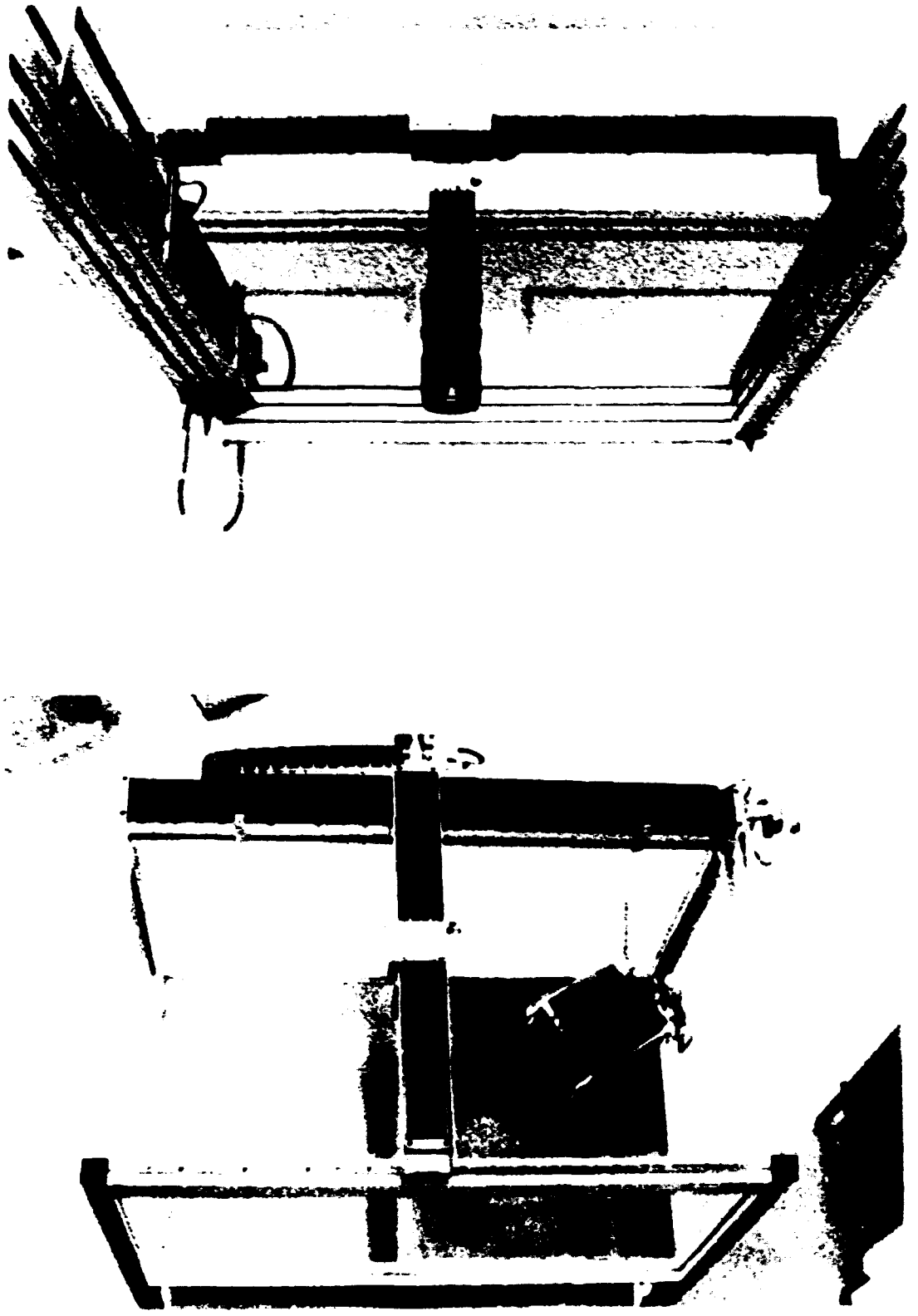

Figure 1. The XY-traversing system.

- The active liquid crystal display (LCD) matrix is fabricated on a silicon substrate.
- The pixel size and the pitch are 50 μm.
- The contrast ratio should be better than 1:60.
- The electronic drivers are attached to the silicon substrate.
- The optical quality of two SLMs should be better than $\lambda/10$.
- The efficiency of the SLMs should be better than 80%.

MRI is producing the LCD matrix with the electronic drivers, and Risø is responsible for the video interface. The most significant technical problems in this task have been the electronic drivers on the SLM. Despite the availability of data sheets on components from Japanese producers, it has not been possible to purchase any such components. It has therefore been necessary to design a special driver configuration where the SLMs are split into four parts each driven in parallel. The design will fulfil the specifications and, when more advance components are available, can be used to get higher video input rates than the usual TV-frame rate. A second problem has been the optical quality of the SLM. For display purposes this is not a major problem, but for Fourier space applications the quality is critical. The LCD substrate will be covered and index matched to a planar glass plate ($\lambda/10$ quality).

2.4.4 Machine Stereo Vision

(A. Skov Jensen, E. Rasmussen, and E. Eilertsen)

Stereodepth perception (stereopsis) was explained and invented by Wheatstone in 1838 and has since been used in various optical instruments. Stereopsis relies on the shift along the line of sight between local areas in the two eyes. The aim of this project is to propose a 3D stereoscopic machine vision system based on a simple correlation scheme that can be implemented optically or electronically and works in real time, i.e. at TV frame rate or faster. Two images have to be recorded with two displaced CCD cameras. The relevant information in the two images is local shifts that can be found by detecting the shift in the peak of the local correlation function.

The present work is performed in cooperation with Alexander G. Sobolev, Institute of Cybernetic Problems (ICP), The Russian Academy of Science Russia, and is supported by a small NATO grant. ICP is working on acousto-optic (AO) correlators later to be interfaced with the stereo videocameras. Calculations show that stereo images can be converted to 3D images at TV frame rate or faster by the use of AO-correlators. A prototype of an AO-correlator has been tested on stereo images by V. Volkov (ICP) at Risø. The experiments were carried out without the proper interface to the videocameras, by the use of video frame grabbers. Approximately ten delays were available in the correlator due to a low input speed of the signals to be correlated. Despite this, reasonable results were obtained. This work will later be reported in detail.

Very convincing results have been obtained by computer simulation, where the parameters for the correlation process can be chosen more freely. Figure 1a shows the 3D results from a set of recorded stereo images of five pencils displaced along a line. Local correlation has been done on the vertical lines in the two images in local segments of 32 pixels. Each correlation is shifted one pixel relative to each other giving considerable overlap. The correlation between two segments can be performed in various ways. Here, one of the segments has been truncated in

order to avoid boundary problems and to separate the correlation scale and increase the depth resolution of the system. This can also be implemented in an AO-correlator. For each correlation function the maximum peak position is found and thresholded. If the peak exceeds the threshold, the 3D image is given a colour (grey tone) equal to the detected shift and, otherwise, the colour is set to the background colour. The thresholding and the truncating technique in Fig. 1b give an edge enhanced 3D image of the pencils.

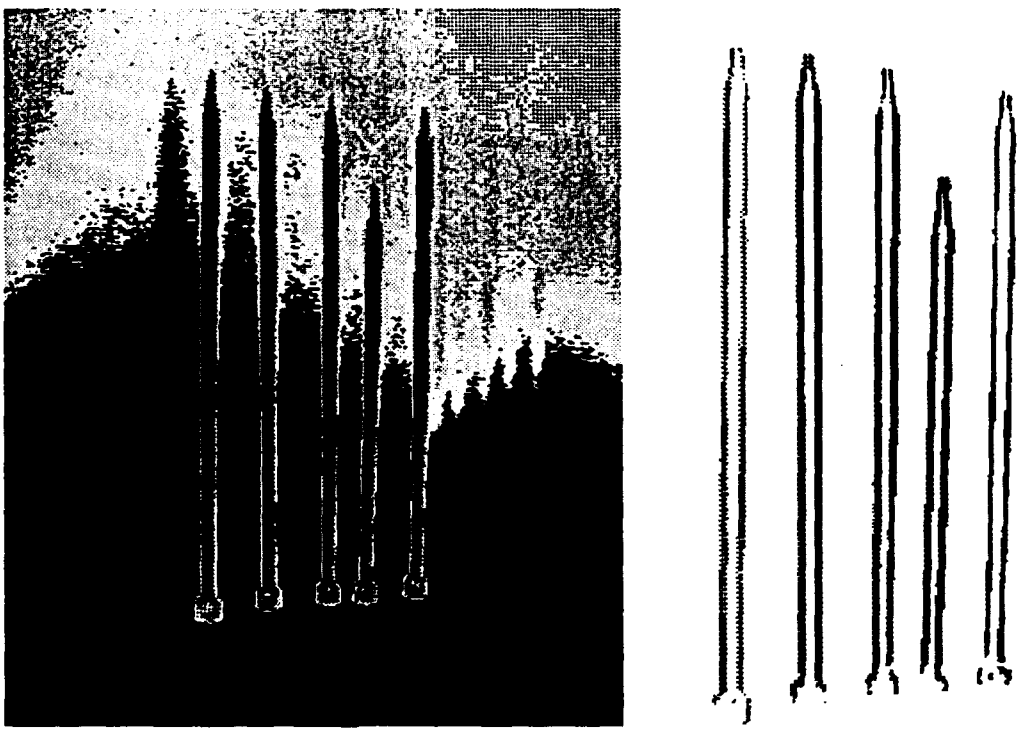

Figure 1a. One of the stereo images. It is seen that a large number of substructures is present besides the images of the five pencils. Figure 1b. The result of the local correlation of the two stereo images. The image is a screen dump from a 16-colour screen. The actual grey levels are difficult to see in this representation, but they cover a range of 16 levels from left to right in the image. The steps in the levels are approximately linearly distributed. Compared with Fig. 1 it is seen that the contour of the pencils is well represented.

2.4.5 Automatic Pig Evisceration - 3D Image Analysis

(S. Sloth Christensen)

The department participates in an EU BRITE project together with the Danish Meat Research Institute, DK (co-ordinator of the project), Siemens AG, D, Ricardo Hitec, GB, and University of Bristol, GB. The purpose of the project is to develop an automatic pig evisceration system. It is the task of Risø to develop and implement the required image processing methods.

The large biological variations between pigs complicate the recognition task considerably. The image processing is therefore based upon an artificial neural network in order to obtain the required precision and noise immunity.

3D information is generally required in order to generate control signals for a

robot. This information is obtained by a 3D sensor system produced by Siemens.

Risø has extended the neural network image processing model to incorporate the 3D information. A number of features are only recognisable if 3D information is present, e.g. a tilted white square on a white background. It is, however, not sufficient to use only the 3D information. Risø has therefore developed a model for sensor fusion that enables the neural network to integrate 3D and 2D image information. This concept provides a flexible and reliable method for identification of feature points in 3D space.

The 3D/2D image processing method has been integrated with the Siemens equipment and is used to generate control signals for the robot.

2.4.6 Neural Network Hardware for Image Processing

(S. Sloth Christensen and A. Andersen (Engineering and Computer Department))

A neural network PC expansion board has been developed in collaboration with the Engineering and Computer Department. The board is among the fastest neural network implementations in the world. It is possible to perform 5,000 classifications/sec with 32 output classes using the standard configuration. It is possible to configure the board to perform 10,000 classifications/sec if the task is simple.

The high classification speed provided by the hardware implementation makes it feasible to apply neural networks to image processing tasks. The enormous amount of data has been one of the major obstacles in applying neural network methods to image processing tasks. The availability of a fast neural network implementation is therefore a crucial step forward in the application of neural networks to real world problems.

The neural network board has already been successfully applied to the recognition of feature points on pig carcasses (BRITE B/E 4152). The capability of performing a large number of classifications within a short time frame has increased the precision and reliability of the system.

3 Continuum Physics

3.1 Introduction

The research areas of the Continuum Physics Section cover studies of fundamental problems in fluid dynamics and aerodynamics as well as studies of plasma physics relevant to fusion energy research. All the fusion relevant research is done under the EURATOM-Risø association. The description of all the scientific contributions is in the following divided into two research areas, (1) nonlinear dynamics of continuum systems and (2) fusion plasma physics. The separation is somewhat artificial since the two fields have a high degree of overlapping.

- *Nonlinear dynamics of continuum systems*
  This research area is concerned with theoretical, numerical, and experimental investigations of nonlinear continuum systems. The emphasis of these investigations has been on studies of coherent structures in two-dimensional flows. The nonlinear dynamic evolution of these structures, which can be characterised as localised and long-lived vortices, was studied by a combination of theoretical, numerical, and experimental investigations. A detailed understanding of the physical properties of two-dimensional coherent structures is of great importance to the description of plasma confinement in magnetic fu-

sion experiments as well as to many fundamental problems in aerodynamics and fluid dynamics.

- *Fusion plasma physics*
  This research area includes fusion relevant research which has not already been mentioned under the previous heading. The topics are turbulent transport, nonlinear evolution of instabilities, plasma equilibria, and diagnostics based on coherent scattering. During 1993 the Risø Q-machine, which has been in operation since 1967 and used for experimental studies of fundamental plasma physics, was dismantled.

3.2 Nonlinear Dynamics of Continuum Systems

3.2.1 Simulation of Viscoelastic Fluids

(Bo Gervang)

A Newtonian fluid (e.g. water) shows a linear relationship between stress and rate of deformation. The proportionality constant is the viscosity of the fluid. All other fluids are denoted non-Newtonian fluids of which the viscoelastic fluids are of particular interest in this study. These fluids behave as a Hookean solid when processed at short time scales but as a Newtonian liquid when processed at long time scales.

The flow past a sphere in an infinite expanse of fluid is simulated. This example was suggested at the Sixth International Workshop on Numerical Methods in Non-Newtonian Flow as a benchmark problem for test of different computer codes. The governing equations are discretised using spectral methods, and a domain decomposition is used in order to resolve the steep gradients in the boundary layer. Both the Eulerian and the Lagrangian formulations are tested when solving the hyperbolic stress equations. Conventional discretisation methods (finite difference, finite volume, and finite element) have only solved the equations for small values of the Deborah number whereas we can, by use of spectral methods, solve the equations for larger values of the Deborah number. The Deborah number may be interpreted as the ratio of the magnitude of the elastic forces to that of the viscous forces.

Formulating the problem in primitive variables - $\mathbf{u}, p, \mathbf{T}$ (velocity, pressure, stress) - gives rise to the solution of the time dependent Stokes operator at each time step. Optimal spaces are sought for both velocity and pressure fields in order to obtain globally solenoidal velocity fields. The associated discrete matrix is singular and new techniques are developed to solve singular systems arising from spectral discretisation of PDEs with domain decomposition.

3.2.2 Studies of Boundary Layer Formation and Detachment in Two-Dimensional Flows

(E.A. Coutsias (University of New Mexico, USA), J.S. Hesthaven, and J.P. Lynov)

One of the most difficult problems in industrial flow control lies in determining the effects caused by the extremely complex flow patterns generated near material boundaries. Here, boundary layers with high vorticity concentrations are usually formed, and through very irregular bursting events these boundary layers detach from the walls and enter into the main flow leading to turbulence. In most engineering designs these processes are treated in a rather crude, statistical manner. However, through the evolution of high power supercomputers and the development of new analytical and computational techniques direct and detailed studies

of the fundamental flow processes near walls are beginning to be possible.

In our numerical studies of two-dimensional, wall bounded flows we have developed accurate spectral algorithms for various nonlinear, dynamic problems. During the past year several quantitative tests have been carried out in order to test the accuracy of these algorithms. One such test was the solution of the

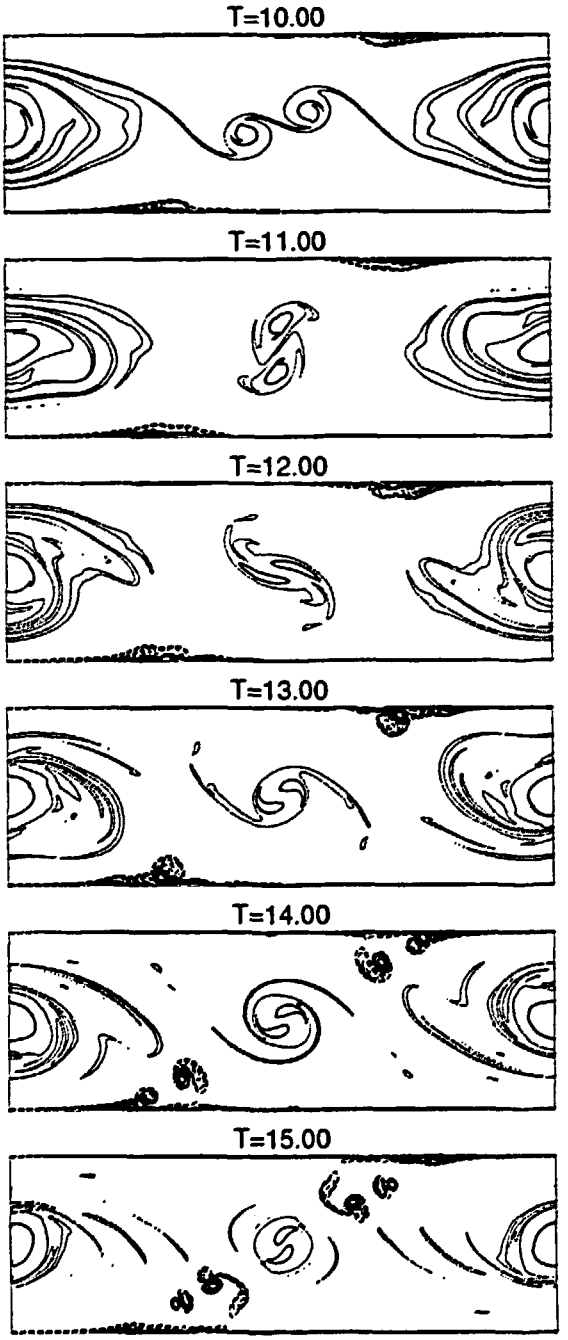

Figure 1. Numerical simulation of shear layer roll-up in a periodic channel with oppositely moving, no-slip walls at Reynolds number 20,000.

Orr-Sommerfeld equation. This is a linear eigenvalue problem which describes the onset of unstable fluctuations in a plane, pressure driven channel flow. In order to solve the eigenvalue problem, our new spectral methods described in section 3.2.3 were employed. As a result of these well-conditioned operators, we were able to determine the eigenvalues with a couple of orders of magnitude higher accuracy than those previously cited in the literature. The results from the eigenvalue problem were subsequently used to check the dynamic behaviour of our full dynamic code with excellent agreement. Similar comparisons between theoretical eigenvalue calculations and fully dynamic simulations were performed for the forced, annular shear layer problem described in section 3.2.4.

Theoretical studies of boundary layer evolution caused by isolated vortical structures have been initiated. The goal of these studies is to provide good, theoretical estimates of the vorticity production and boundary layer detachment caused by vortex-wall interactions. Our initial investigations have been concerned with comparisons between theoretical estimates of idealised, vortex sheet production by incoming point dipoles and the complete boundary layer formation by incoming dipoles with distributed vorticity. These studies have led to the development of new schemes for the initial projection of the vorticity field necessary in order to satisfy the no-slip boundary conditions at the walls at the very start of the simulations.

An example of complex boundary layer behaviour is shown in Fig. 1. Here results from a high resolution simulation (342 Chebyshev and 684 Fourier modes) are shown for a shear layer roll-up in a periodic channel with oppositely moving walls at Reynolds number 20,000. The contour plots show instantaneous vorticity distributions. Boundary layer formation and eruption is clearly seen when main flow vorticity approaches the channel walls.

3.2.3 Development of Accurate and Efficient Numerical Algorithms for the Solution of Problems with Sharp Variations

(E.A. Coutsias*, T. Hagstrom*. and D. Torres* (*University of New Mexico, USA))

The numerical studies pursued in connection with our fluid dynamics research rely critically on certain innovative algorithms that have been developed at Risø and allow the exceedingly accurate solution of boundary value problems for various differential equations.

The dynamics of vortices near walls, the filamentation occurring in the evolution of shear layers or during vortex-vortex interactions, and the analysis of flows exhibiting sharp gradients in flow properties all require the accurate integration of highly nonlinear partial differential equations for very long time. Due to the exponential instabilities and the potential occurrence of chaotic events in such problems, very high accuracy must be maintained throughout the computations.

In our efforts to maintain a very high standard of accuracy and reliability in our simulations, we have relied on the excellent approximating power of spectral families, such as Chebyshev polynomials. The general idea in these methods is the expansion of the quantities involved in terms of classical orthogonal polynomials. Then, differential operators are expressed as matrices acting on the expansion coefficients. In general, these matrices are full and ill-conditioned, and the resulting discretisation of the field equations is quite cumbersome and hard to manipulate, despite its "infinite ord. accuracy". Such manipulations tend to be prohibitively expensive in terms of computer time.

By taking advantage of certain simple recursion relations and other, apparently not widely known algebraic properties of orthogonal polynomials[1)], we are able to solve large classes of problems, including all the problems occurring in our

various hydrodynamic codes, by computationally simple and well-conditioned algorithms which scale linearly with the number of computational nodes employed in our discretisations. Several test problems that demonstrate the power of the new techniques have been solved. For example, in a problem including an internal shock wave our method allows the same accuracy to be obtained by the use of as few as 64 modes as a traditional approach would by using $\approx 32,000$ modes[2].

Special attention needs to be given to the analysis of problems in geometries involving coordinate system singularities. In this direction we have been successful in overcoming the difficulties associated with the spectral solution of the Poisson equation in a disk, an essential first step towards developing a fast and accurate Navier-Stokes solver for flows in circular domains. This will be needed for our studies in connection with the projected parabolic rotating tank experiments that are in the construction phase at Risø.

1) Coutsias, E.A. (1993), submitted to SIAM J. of Sci. Stat. Comp.
2) Coutsias, E.A., Hagstrom, T., and Torres, D. (1993), submitted to Math. Comp.

3.2.4 Numerical and Analytical Studies of Transitions in Circular Shear Layers

(K. Bergeron*, E.A. Coutsias*, J.P. Lynov, and A.H. Nielsen (*University of New Mexico, USA))

The evolution of circular shear layers provides a rich backdrop for investigations of the transition to turbulence in fluids and plasmas. A better understanding of the processes involved can lead to finer methods for influencing, even controlling, this complex phenomenon. The Kelvin-Helmholtz instability of shear lavers offers a generic pathway for the formation of coherent vortical structures which in recent years have become recognised as the main actors in many situations in which traditional analyses of turbulence have proved inadequate. An interesting example is offered by the problem of vortex shedding from structures that are responsible for such common phenomena as jet airplane noise, catastrophic failures of large structures under strong wind loads, and transonic flight control.

The quantisation inherent in circular geometry leads to the formation of well-defined vortical braids, unlike the incessant pairing and scale evolution of planar shear layers. Both cylindrical, magnetised, electrostatic plasma experiments and rotating fluid experiments have produced rich bifurcation sequences of different symmetries, as well as oscillating, quasi-periodic, or chaotic states. We have pursued numerical and analytical studies which demonstrate that such transitions can be accurately described by reducing the governing slightly viscous, forced Navier-Stokes equations to a system of ordinary differential equations of few degrees of freedom. The simplest case studied in detail so far leads to an equation of the Landau type describing the saturation of the Kelvin-Helmholtz instability in terms of the amplitude $A(\tau)$ of the most unstable mode, with τ a slow time scale. In this case the dynamic equation assumes the form:

$$\alpha A_\tau = \beta A + \gamma A^2 A^*.$$

The (complex) coefficients of the reduced equations are computed by numerical solution of appropriate eigenvalue problems; the resulting time evolution is in excellent agreement with direct simulations of the flow, and both sets of calculations faithfully reproduce experimental observations of circular shear layer transitions in the split annulus experiment[1].

The two approaches supplement each other in predicting the transition to states of ever increasing complexity, even beyond the regimes that have so far been experimentally accessible.

A direct practical application of this work, besides the understanding that it will produce the transition mechanism in circular shear layers, can be better understanding of flows in computer disk drives. Similar bifurcation phenomena have been observed in circular flames[2] and it will be interesting to carry out a comparison of the transition mechanisms at work in the two problems.

Ultimately, this extremely accurate reduction of the phenomenon to low dynamic system behaviour offers the promise of controlling the transitions by proper application of external forcing. An investigation of various methods of applying controlling forces to this flow is planned.

1) Chomaz et al. (1988). J. Fluid Mech. 187, 115-140.
2) Bayliss, Leaf, and Matkowsky (1993). Comb. Sci. Tech. to appear.

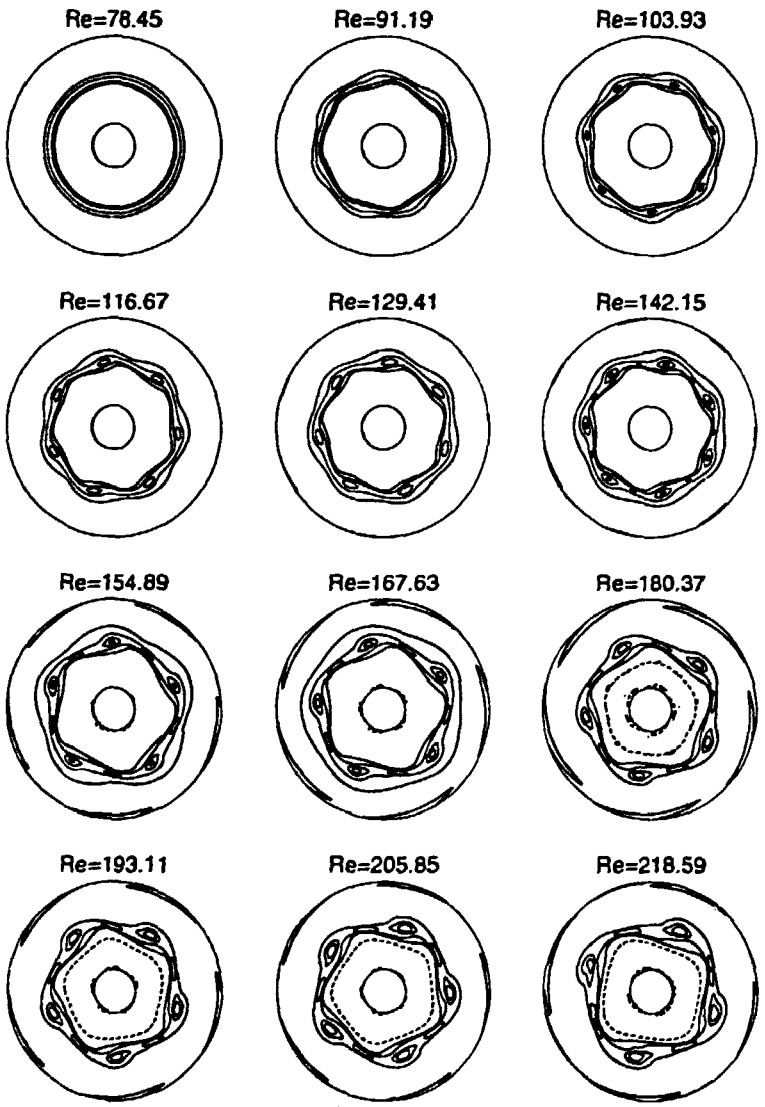

Figure 1. Numerical simulation of an annular shear layer with slowly increasing forcing. The contour plots show instantaneous vorticity distributions. A small amount of noise was added to the initial, rotationally symmetric, vortiey distribution. At the critical Reynolds number, the flow makes a transition to a state with azimuthal mode number m = 7. As the Reynolds number is increased further, the flow undergoes a sequence of symmetry breaking bifurcations to states with lower values of m.

3.2.5 Multidomain Spectral Simulation of Unsteady, Compressible Flow Around a Circular Cylinder

(J.S. Hesthaven, W.S. Dons*, D. Gottlieb* (* Brown University, Division of Applied Mathematics, Providence, RI 02912, USA), and M.D. Salas** (** ICASE, NASA Langley Research Center, Hampton, VA 23665, USA))

The behaviour of compressible flow past a circular cylinder has been used as a model for fundamental studies of external flows. In spite of the simplicity of the geometry, this simple flow embodies a variety of interesting flow phenomena, ranging from steady Stokes flow to viscous wake flow and fully developed turbulence.

During the last decades the dynamics of unsteady, compressible wake flows past a cylinder have been studied intensively - experimentally as well as theoretically. Recent experiments seem to indicate that coupling to acoustic waves propagating upstream may have a significant impact on the overall dynamics of the flow. These acoustic waves may appear in wind tunnel experiments, where the turbine generates sound waves which propagate downstream, reflect at the end of the wind tunnel and, finally, propagate upstream where they may interfere with the experiment.

In order to study this phenomenon, we have developed a pseudospectral Fourier-Chebychev code, where the computational domain is split into several nonoverlapping subdomains. This allows larger flexibility in choice of grid, grid mappings, and filtering. The artificial outer boundary is treated by employing the method of characteristics for hyperbolic systems of conservation laws, thereby assuming that the flow may be considered inviscid at the outer boundaries. Matching of characteristic waves has also been employed as a patching scheme between the nonoverlapping subdomains. The code can handle flows with Mach number < 0.6 and Reynolds number < 200, where three-dimensional effects become important.

As an example, in Fig. 1 we see the full computational domain, consisting of three nonoverlapping subdomains used for simulating the flow past a cylinder at $M = 0.4$ and $Re = 108$. In Fig. 1 we also show a contour plot of the relative density ρ/ρ_∞. The formation of the Von-Karman street is clearly demonstrated and the Stroudal number for the shreading is found to be $St = 0.16$, in full accordance with experimental findings. These results clearly demonstrate the applicability of the domain patching and the outer boundary conditions.

The formulation of the scheme as a multidomain approach lends itself to parallel implementation of contemporary parallel coarse-grained architectures. Indeed, we observe a speedup of 1.8 at a two-processor system, illustrating the effectiveness by which such problems may be solved when employing modern computational approaches.

In accordance with the experimental findings, we observe that acoustic waves corresponding to a relative pressure perturbation as low as 0.1 % may indeed have a significant impact on the shedding dynamics. However, we also find that heating the cylinder may have an even greater impact on the dynamics. These results are of importance to understanding measurements obtained in wind tunnels by using hot wires.

We plan to conduct a thorough investigation of the effects of the acoustic waves and the heating of the cylinder in order to uncover these new phenomena. We also intend to improve the computer code by employing recent theoretical results which ensure temporal stability of the computational scheme, thus allowing for longtime integration of the governing equations.

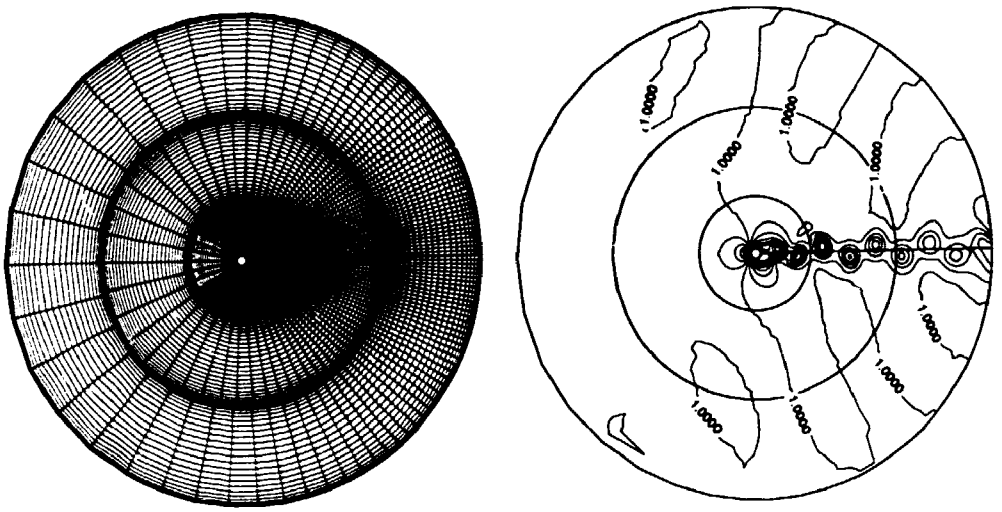

Figure 1. Computational grid and relative density, ρ/ρ_∞ at $T = 156.21$ for a three-domain simulation of a compressible flow past a cylinder at $M = 0.4$ and $Re = 108$. The Stroudal number, based on the shreading frequency of the vortices and the diameter of the cylinder, is $St = 0.167$.

3.2.6 Linear Stability of a Modon on the β-Plane

(J.S. Hesthaven, J. Nycander (Uppsala University, Uppsala, Sweden), and J. Juul Rasmussen)

In recent numerical studies it has been shown that modons seem to be linearly unstable, even in parameter regimes where they are known to be nonlinearly stable, i.e. eastward propagating. This counterintuitive result has been obtained for studies of modons in a full spherical geometry. However, due to the complexity of the geometry, the convergence of the growth rate with increased spatial resolution was poor, and one may speculate if the linear instability observed is a numerically induced phenomenon.

In order to study this problem, we have developed a model that allows studies of the linear stability on the β-plane by using a time integration technique, as opposed to solving the full two-dimensional eigenvalue problem. The simplicity of the β-plane geometry allows the use of sufficient spatial resolution to gain confidence in the results.

The model is based on a linearisation of the quasi-geostrophic equivalent barotropic equation in a moving reference frame, and an initial perturbation with an energy spectrum $E(k) \sim k^{-3}$ and random phase. As spatial interpolation scheme we used a double periodic spectral scheme and as temporal integration scheme we employed a third order Adam-Bashforth method.

Our study shows good conformity with the results obtained for the full spherical geometry. Although we see slight differences introduced by the differences in geometry, frequency, and growth rate for the most unstable mode, our study clearly confirms the linear instability of the modon.

Careful inspection of results obtained in other studies indicates that the linear instability corresponds to an azimuthal twisting of the structure. This result was also found for the spherical case. However, it is well known that the modon is

nonlinearly stable to azimuthal perturbations. This suggests that the linear instability is saturated by nonlinear effects which dominate the dynamics for larger azimuthal perturbations. Indeed, in full nonlinear simulations we observe that for small initial angular perturbations the azimuthal twisting initially grows exponentially, but soon the nonlinear saturation decreases the growth rate to such an extent that the modon, finally, propagates as expected from conservation of potential vorticity.

3.2.7 Dipole Formation from Breaking Rossby Waves

(G.G. Sutyrin*, I.G. Yushina* (*P.P. Shirshov Institute of Oceanology, Moscow, Russia), J.S. Hesthaven, J.P. Lynov, and J. Juul Rasmussen)

Large-scale quasi-two-dimensional flows in planetary atmospheres and oceans are known to be highly anisotropic due to the variation of the Coriolis parameter with the latitude, the so-called β-effect, which allows the propagation of Rossby waves. In a magnetised plasma the inhomogeneity of the plasma density gives rise to similar effects and allows the propagation of drift waves. The understanding of the nonlinear dynamics of Rossby waves and drift waves together with the associated transport has important implications on both applied and fundamental atmospheric and oceanic research as well as on fusion research.

Abundant intense vortices in the atmospheres and oceans are capable of generating large amplitude Rossby wave patterns and their interaction with the vortices may strongly affect the general dynamics. A general feature of the evolution of a strong monopolar vortex on the β-plane is that during the meridional propagation of the vortex it reorganises into a tripolar structure with an elliptical core with vorticity of the same sign as in the original monopole and two satellites with opposite vorticity[1]. Rotation and distortion of the satellites lead to increased mixing near the boundary of the vortex core providing a mechanism for fluid exchange between the vortex core and the generated wave wake field.

Further investigations based on numerical solutions of the quasi-geostrophic equivalent barotropic equation (the so-called Hasegawa-Mima equation in the plasma context) have indicated that there is a critical value for the vortex intensity below which the satellites do not appear. For these intermediate intensities the coupling of the vortex and its wave wake is found to lead to the appearance of large-scale dipole vortices from the breaking of the waves. The dipole will in turn interact with the original monopole vortex leading to increased meridional displacement of the vortex core and providing additional fluid transport. Detailed numerical investigations for a variety of parameters have been conducted to reveal the mechanism of the Rossby wave breaking and the dipole-monopole interaction.

1) Hesthaven, J.S., Lynov, J.P., Rasmussen, J.J., and Sutyrin, G.G. (1993). Phys. Fluids A 5, 1674-1679; Sutyrin, G.G., Hesthaven, J.S., Lynov, J.P., and Rasmussen, J.J. J. Fluid Mech. in press.

3.2.8 Dynamics of Nonlinear Dipole Vortices

(J.S. Hesthaven, J.P. Lynov, A.H. Nielsen, J. Juul Rasmussen, M.R. Schmidt* (*University of Odense, Denmark), E.G. Shapiro** and S.K. Turitsyn** (**Institute of Automation and Electrometry, Novosibirsk, Russia))

Stationary solutions to the Euler equations describing two-dimensional flows have a functional relationship between the vorticity, ω, and the stream function, ψ, i.e. $\omega = f(\psi)$ (ω and ψ are related by $\omega = -\nabla^2\psi$). For the simplest case, where f is a linear function one finds, for instance, the so-called Lamb dipole which often

appears to be a good approximation to dipoles found in experiments in rotating or stratified fluids. We have numerically found a steadily propagating dipole with a strongly nonlinear relationship between ω and ψ, with $f(\phi) = \alpha\phi + \beta\phi^3 + \gamma\phi^5$ inside a separatrix of almost circular shape and $f(\phi) = 0$ outside the separatrix, "a nonlinear dipole"[1]. Here ϕ is the stream function in the frame moving with the dipole. A similar type of dipole has also been found in experiments under certain conditions. We have investigated the nonlinear dynamics of this dipole numerically. In Fig. 1 we show an example of a head-on collision between two nonlinear dipoles. The two dipoles approach each other, change partners and, finally, two "new" dipoles propagate away in the direction perpendicular to the initial direction of propagation. The two "new" dipoles are identical to the two initial ones. Thus, the dipoles are stable to head-on collisions, as is the Lamb dipole. We have also revealed that an off-axis collision between two nonlinear dipoles may lead to the formation of a tripolar structure, as also found for Lamb dipoles. Making the nonlinear dipole collide head-on with a Lamb dipole, we found that both types of dipoles regenerated after the interaction and continued to propagate along their original direction away from each other.

1) Hesthaven, J.S., Lynov, J.P., Michelsen, P., Nielsen, A.H., Rasmussen, J.J., Schmidt, M.R, Shapiro, E.G. and Turitsyn, S.K. (1993). Risø-R-674, p. 38.

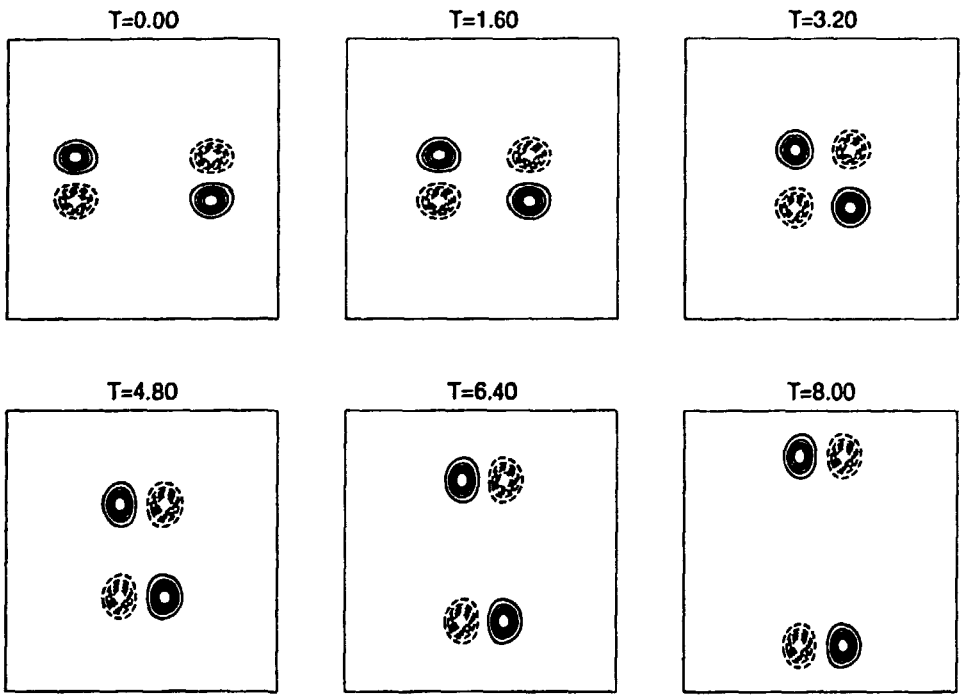

Figure 1. Contour plots of the vorticity showing the head-on collision of two nonlinear dipoles.

3.2.9 Interaction of Dipolar Vortices with Cylinders

(E.A. Coutsias (University of New Mexico, USA), J.P. Lynov, A.H. Nielsen, J. Juul Rasmussen, and B. Stenum)

The dynamics of dipolar vortices colliding with cylinders are investigated both numerically and experimentally. In the numerical investigations we employ a fully dealiased, spectral scheme based on Fourier-Chebyshev expansions. This allows very high resolution of the boundary layers. The flow field is governed by the two-dimensional Navier-Stokes equation

$$\frac{\partial \omega}{\partial t} + \mathbf{v} \cdot \nabla \omega = \nu \nabla^2 \omega \ .$$

The velocity is given as $\mathbf{v} = \nabla \psi \times \hat{z}$, ψ being the stream function, the vorticity as $\omega = -\nabla^2 \psi$, and ν is the kinematic viscosity. The flow is subject to no-slip conditions so that it matches the wall velocity at the boundaries. In the numerical studies a Lamb dipole was used as the initial dipolar structure and was made to collide with cylinders of various radii relative to the radius of the dipole.

The results of the numerical investigations were compared with experimental investigations performed in a rotating tank with water (see section 3.2.10). Here the dipolar vortices were generated by injection of dyed jets and made to collide with cylindrical obstacles of different radii. Using the parameters (size and velocity) of the well formed dipoles in the experiment - dipoles which are quite similar to Lamb dipoles - as input to the numerical investigations, we revealed detailed agreement between the numerical and experimental results. The interaction is summarised as follows: as the dipole approaches the cylinder, it induces opposite sign wall vorticity layers. These grow and at a minimum approach the wall layers roll up into tight secondary vortices which couple to the opposing primary lobes. In turn the combined structure detaches from the cylinder thereby splitting the primary dipole into two.

In further numerical investigations we attempted to find a lower limit of the cylinder radius, below which the splitting of the incoming dipole would not occur. For axial collisions we have not found that limit within the possible resolution of the numerical scheme. For a cylinder diameter D_c of 1/64 of the dipole diameter D_d, we still observe a splitting as seen in Fig. 1. Note, however, that the original dipole reforms behind the cylinder and propagates away; for larger cylinders it rejoins in front of the cylinder and collides with it again. For off-axis collisions with small cylinders the dipoles were only weakly perturbed and found to reconstruct after the interaction, which agrees with our experimental findings. In addition, from the numerical investigations we observed that the total generated vorticity in the upper half-plan is almost independent of the cylinder radius in the investigated interval ($1/64 \geq D_c/D_d \leq 1$). This is illustrated in Fig. 2, where the time evolution of this generated vorticity is shown for different radii.

In order to further validate our numerical scheme we have initiated a detailed comparison with the results obtained by the group at the University of Rome, Italy[1]. They have made similar investigations by employing a quite different numerical model based on a finite difference scheme. Preliminary comparisons indicate that our spectral scheme is more accurate than the finite difference scheme, in particular for higher Reynolds numbers ($\geq$ 1000).

1) Orlandi, P. (1990). Phys. Fluids A2, 1429-1436; (1993). Phys. Fluids A5, 2196-2206.

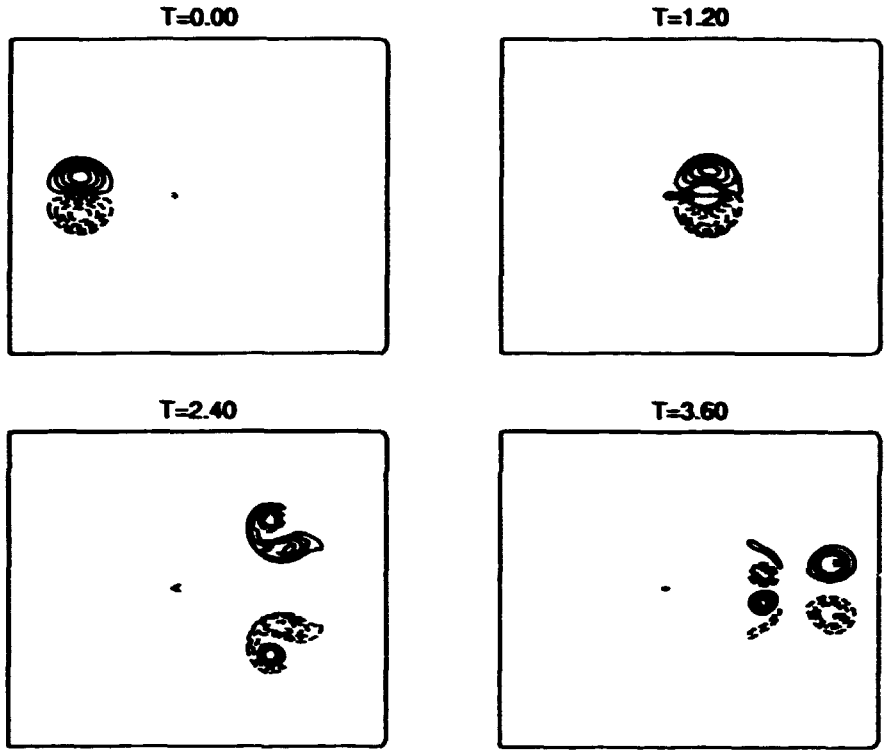

Figure 1. Interaction of a dipolar vortex with a small cylinder of diameter 1/64 of the dipole diameter.

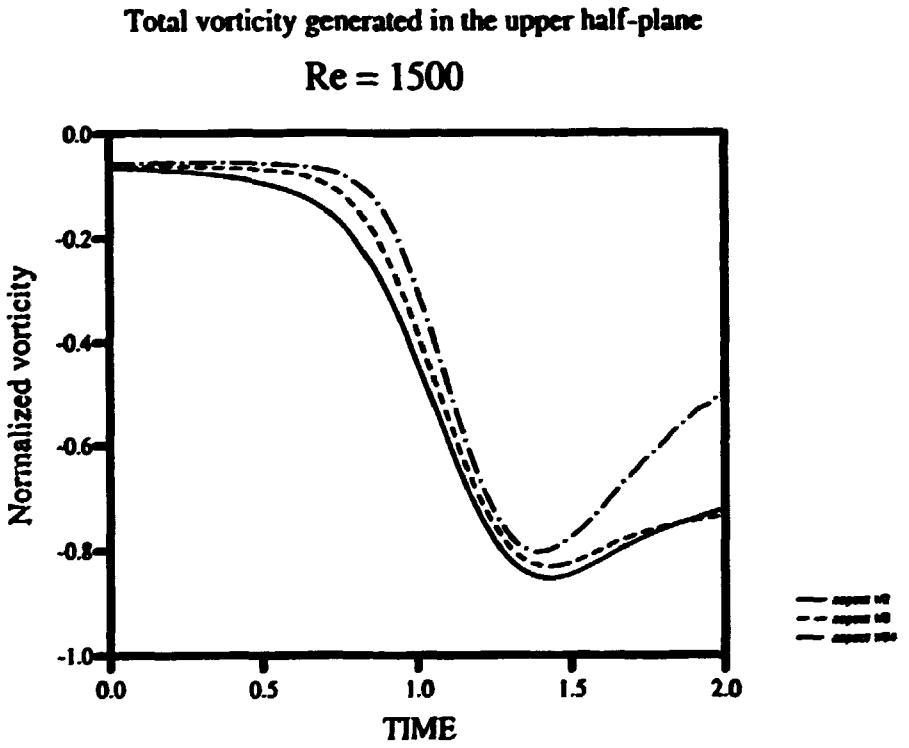

Figure 2. The time evolution of the total negative vorticity generated during the interaction of the dipole with the cylinder for different values of D_c/D_d.

3.2.10 Experimental Studies of Dipole Interaction with Walls in 2D Flows

(M. Nielsen, J. Juul Rasmussen, and B. Stenum)

Coherent structures appear in two-dimensional (2D) as well as three-dimensional (3D) flows. In particular, the formation of coherent vortex structures is likely in 2D flows as a result of self-organisation during the inverse energy cascade characterising these flows. In this way momentum transfer to a 2D system as a rotating fluid often results in the formation of stable, isolated vortex dipoles[1].

In order to perform detailed studies of such dipoles colliding with curved and straight walls we have applied the DigImage particle tracking velocimetry facility[2] in the rotating tank setup.

The setup consists of a turntable rotated with an angular frequency of 0.63 Hz. Onto this table a water filled (15 cm depth) square tank with side walls of length 1 m and flat bottom is placed. In the tank the various wall structures are placed. The dipoles are produced by injection of well-defined jets. In order to produce symmetric dipoles a movable plate is placed in front of the nozzles. Typically, dipoles with a diameter of about 20 cm and a propagation speed of about 1 cm/s are formed. The tank is surveyed by a video camera following the rotating system and coupled to a videotape recorder and a monitor via a set of slip rings.

Small particles with densities smaller than those of the fluid have been added to float on the surface, are illuminated from the top, and the experiment is recorded on a videotape recorder. In the subsequent image processing and analysis the video frames are digitised one by one, and the particles are localised and matched to each other from one frame to the next. In this way the particle tracks and hence the velocity field and its evolution can be determined. However, it turned out that particles floating on the surface tend to make clusters in time scales of the same order as the experimental time scale due to the surface tension. Although a large number of different particles and reduction of the surface tension with chemicals have been applied, the clustering was found to influence the particle tracking significantly. In addition, it was found to be difficult to control the detailed formation of the dipoles in the rotating fluid and hence make reproducible experiments. Therefore, we have started experiments in stratified fluids instead. In stratified fluids the particles are floating in one layer on a depth corresponding to the density of the particles. The particles are consequently not influenced by the surface tension.

A two-tank system for making stratified fluids and a tank (80 cm x 60 cm) for the experiments have been built. Preliminary studies have shown that the particle tracking is working well in the stratified system.

1) Kloosterziel, R.C. and van Heijst, G.J.F. (1991). J. Fluid Mech. 223, 1.
2) Dahiei, S.R (1992). Applied Scientific Research 49, 217.

3.3 Fusion Plasma Physics

3.3.1 Experimental Investigations of Two-Dimensional Plasma Turbulence

(A.H. Nielsen, M.O. Nielsen, H.L. Pécseli (University of Oslo, Norway), and J. Juul Rasmussen)

The experimental investigations of low frequency, flute-type plasma turbulence were concluded. The investigations were performed in the Q-machine plasma. The Q-machine has now been closed down and dismantled.

The fluctuations were generated by the Kelvin-Helmholtz instability due to

a strongly sheared azimuthal flow of the residual plasma surrounding the main plasma column. The radial potential variation in the residual plasma and thereby the azimuthal flow could be controlled by the bias of a limiting aperture inserted perpendicularly to the plasma column. In the last phase of the investigations we concentrated in particular on a detailed analysis of the anomalous plasma transport associated with the turbulence.

In order to monitor the turbulent transport we measured the fluctuations in density, $\tilde{n}$, obtained from the ion saturation current, j_i, to a Langmuir probe and the azimuthal electric field component, $\tilde{E}$, obtained from the floating potential difference, V_{fl}, measured at two closely spaced Langmuir probes. It should be noted that if there are significant fluctuations in temperature, $\tilde{T}_e$, one cannot directly deduce $\tilde{n}$ and $\tilde{E}$ from j_i and V_{fl}, respectively, but has to account for $\tilde{T}_e$. Analysing the resulting radial flux: $\tilde{\Gamma}(t) = \tilde{n}(t)\tilde{E}(t)/B_0$, we obtained detailed information about the plasma transport that can be attributed to the turbulent fluctuations. We interpreted our observation as an indication of the transport in our experiment being a mixture of Brownian type turbulent diffusion and sporadic bursts. By employing a conditional sampling technique to the spatially varying potential and density fluctuations with the flux signal as reference signal, we verified that the bursts in the flux corresponded directly to the presence of coherent vortical structures.

It was explicitly demonstrated that the largest amplitude vortices were actually very effective in transporting plasma, but they occurred so rarely that their accumulated effect was small compared with that of their small amplitude counterparts[1].

The radial dependence of the averaged value of $\tilde{\Gamma}$, Γ_0, as well as that of the fluctuation levels of both $\tilde{E}$ and $\tilde{n}$ were measured simultaneously for varying conditions. We found that Γ_0 had the maximum value at a radial position just outside the main plasma column. For larger radii Γ_0 decreased monotonically almost as $1/r$, where r denotes the radial position. However, the absolute magnitude of Γ_0 did not appear to be correlated with the absolute fluctuation level and the position of the maximum of Γ_0 was usually not coinciding with the position of the maximum fluctuation level, as would be expected from considerations based on quasi-linear theory. This is indicated in Fig. 1 where we have plotted the cross-coherence, γ, defined as:

$$\gamma = \frac{\Gamma_0}{\sqrt{<\tilde{E}^2><\tilde{n}^2>}/B_0}$$

for three different values of the magnetic field. These findings are consistent with the observation that the evolution of the turbulence is dominated by coherent structures. It is, strictly speaking, not meaningful to associate a diffusion coefficient with the transport process described above. However, defining an "effective" diffusion coefficient as $D = \Gamma_0/|\nabla n_0|$ we find that even if there is a clear tendency for D to decrease with increasing B_0, our results are not clearly consistent with the Bohm-scaling $D \propto 1/B_0$. Furthermore, we found that the total turbulent flux, Γ_0, is consistent with the effective particle flux that can be derived from the density gradient in the residual plasma. Thus, far the dominating transport is fluctuation driven transport. This is also found in the "scrape-off layer" of a Tokamak plasma[2].

In order to assess the importance of possible temperature fluctuations on these measurements we have measured the temperature fluctuations directly in the residual part of the plasma by means of the triple-probe method[3]. We found that the relative level of temperature fluctuations was below 0.1 which is somewhat lower than the relative density fluctuation level and the normalised potential fluctuation level. Furthermore, we found that $\tilde{T}_e$ is almost in phase with $\tilde{n}$ as is seen from the

cross-correlation $< \tilde{n}(t)\tilde{T}_e(t+\tau) >$ shown in Fig. 2. This implies that the "error" on our fluxes obtained without correcting for the temperature fluctuations would be below 20%.

1) Huld, T., Nielsen, A.H., Pécseli, H.L., and Rasmussen (1991). J.J., Phys. Fluids B3, 1609-1625; Nielsen, A.H., Pécseli, H.L., and Rasmussen (1992). J.J., Ann. Geophysicae 10, 655-667; Pécseli, H.L., Coutsias, E.A., Huld, T., Lynov, J.P., Nielsen, A.H., and Rasmussen, J.J. (1992). Plasma Physics and Controlled Fusion 34, 2065-2070.

2) Wootton, A.J., Tsui, H.Y.W., and Prager, S. (1992). Plasma Physics and Controlled Fusion 34, 2023-2030.

3) Kamitsuma, M., Chen, S-L., and Chang, J-S. (1977). J. Phys. D: Appl. Phys. 10, 1065-1077.

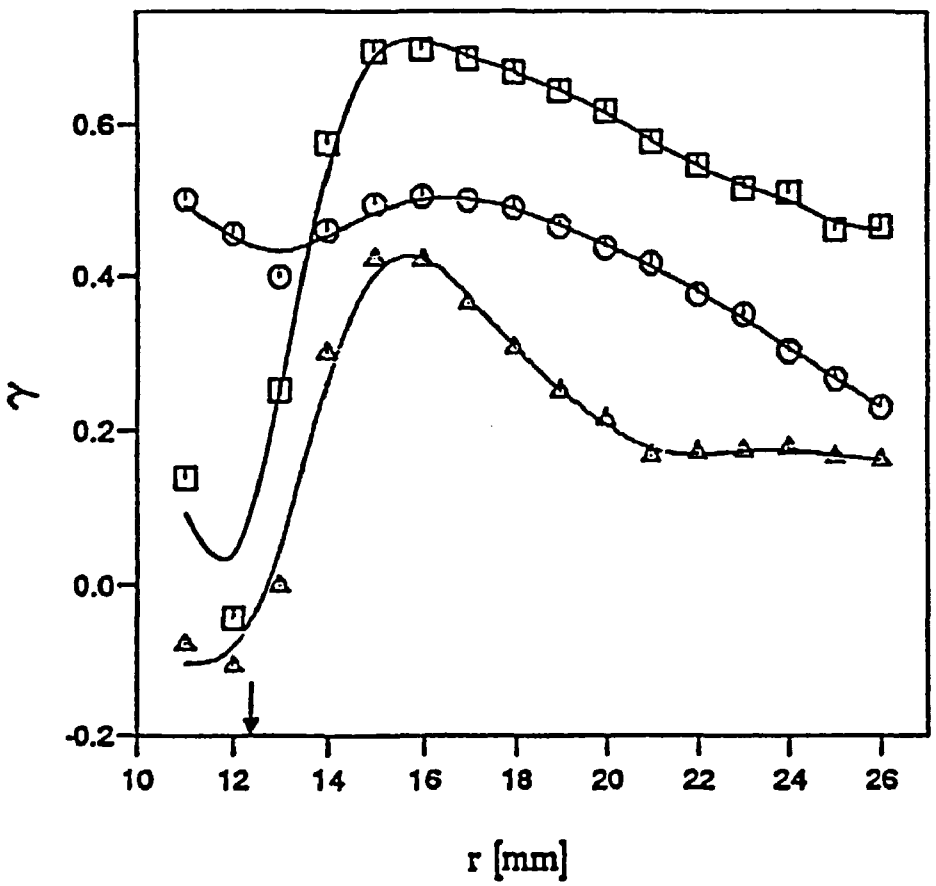

Figure 1. Radial variation of the cross-coherence γ for three different magnetic fields: □ : $B_0 = 0.21\ T$, ○ : $B_0 = 0.28\ T$, *and* △ : $B_0 = 0.42\ T$. *The arrow denotes the edge of the plasma column.*

3.3.2 Experimental Evidence for Mode Selection in Turbulent Plasma Transport

(A.H. Nielsen, H.L. Pécseli (University of Oslo, Norway), and J. Juul Rasmussen)

In the experimental investigations of low frequency turbulence in the Q-machine plasma we have obtained evidence for the simultaneous presence of two types of oscillations. One type has the characteristics of drift waves - i.e. the density fluctuations, $\tilde{n}$, are in phase with the potential fluctuations, $\tilde{\phi}$; the relative level, $\tilde{n}/n_0$,

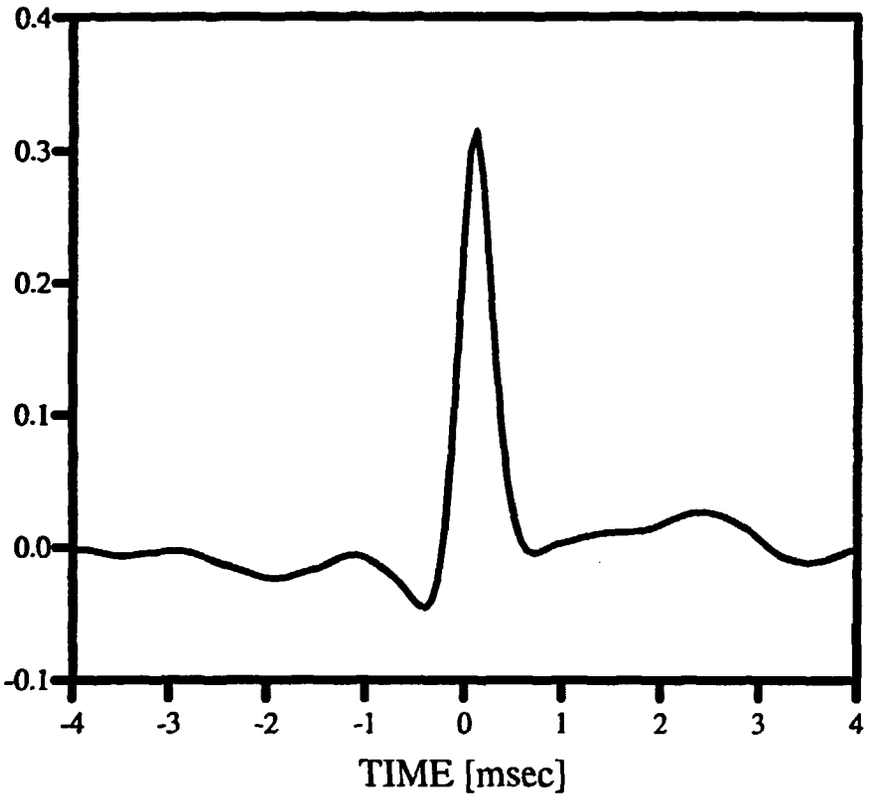

Figure 2. The cross-correlation $\langle \tilde{n}(t)\tilde{T}_e(t+\tau)\rangle$.

is about equal to the normalised potential fluctuation level, $e\tilde{\phi}/T_e$; and the fluctuations propagate with the electron diamagnetic drift velocity. The other type has the characteristics of a flute mode (or convective cell mode) as discussed in section 3.3.1. The two types of modes are distinguished by employing a conditional sampling technique with different conditions applied to the same signal. It is further found that the drift wave type fluctuations do not give any significant contribution to the turbulent transport, while the flute type modes account for the major part of this transport.

3.3.3 Modulational Instability of Plasma Waves in Two Dimensions

(V.I. Karpman (Racah Institute of Physics, Jerusalem, Israel), J.P. Lynov, P. Michelsen, and J. Juul Rasmussen)

The nonlinear evolution of a two-dimensional modulational instability of plasma waves has earlier been shown either to proceed into an approximate exponential growth of wave amplitude or a recurrent type of behaviour in which wave amplitude and density modulation increase and decrease repeatedly. The number of recurrences may depend on initial conditions and on the relevant plasma and wave parameters. In order to understand these processes in more detail we have investigated the evolution by a two-dimensional numerical simulation. As a model we have chosen the equations describing interaction between whistler waves and either fast or slow magnetosonic waves. The equations were solved numerically in

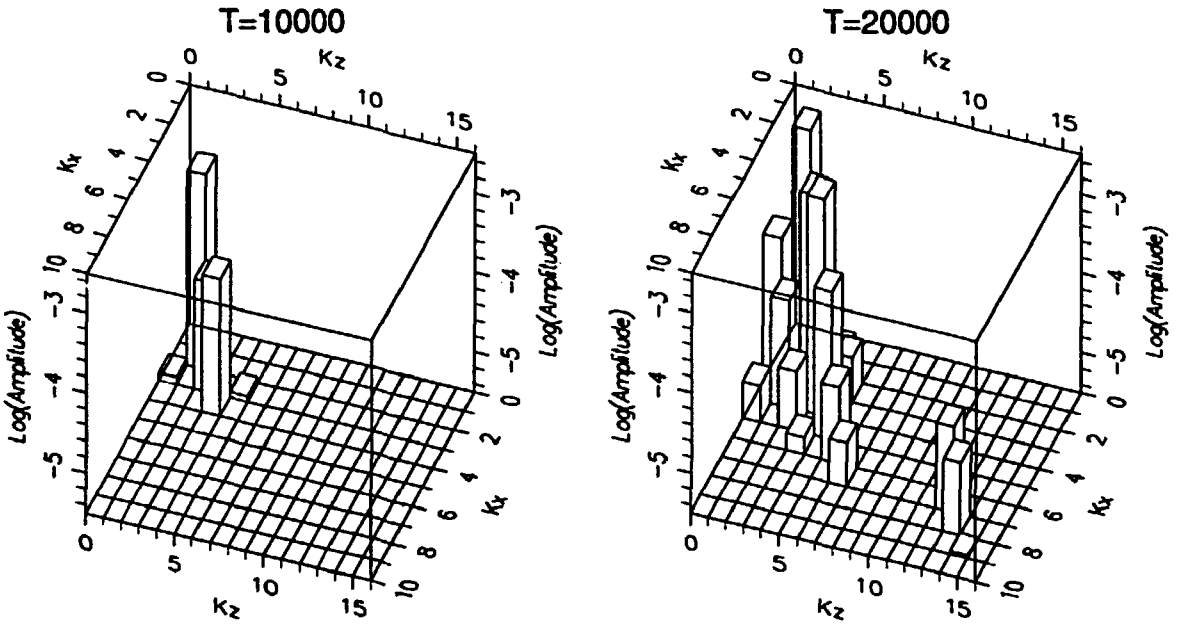

Figure 1. The mode spectrum for the interaction with the fast magnetosonic mode for two different times. Note the growth of the unstable high order modes.

a two-dimensional domain with periodical boundary conditions. We employed a fully dealiased spectral method.

The two cases behave differently. For the case of the interaction with the fast wave, the instability is in general found to evolve in a quasi-recurrent manner in which the main part of the energy resides in the fundamental mode of the initial modulation. For the longtime evolution the energy is spreading slowly to larger and larger wave numbers resulting in a random wave field. As the initial condition the whistler wave is modulated almost perpendicularly to its direction of propagation along the z-axis, i.e. the ratio of the modulational wave numbers, $\alpha = K_z/K_x \ll 1$. This corresponds to the region of modulational instability with the maximum growth rate obtained for a certain α_c. For low amplitudes and $\alpha = \alpha_c$ the evolution shows three clear recurrence periods before the spreading of the energy becomes significant. This behaviour is well described by a simplified model based on a generalised Hamiltonian and truncated to involve only few modes. For increasing wave amplitude the recurrent feature becomes less pronounced and the spreading of the energy to higher modes proceeds faster. For a given amplitude the evolution is found to depend strongly on the value of α, having a maximum of recurrence for α close to α_c. For $\alpha > \alpha_c$ the recurrence first becomes a little better and then worse. However, in this region it is interesting to note that it is important to include a large number of modes (64 x 64 at least) to get the correct result. With fewer modes several additional recurrences show up. For $\alpha < \alpha_c$ the spreading to the higher modes proceeds considerably faster: already for $\alpha = 0.99\ \alpha_c$ only one recurrence period is observed. The observed features may be qualitatively explained from knowledge of the dispersion relation and growth rate of the linear waves. In Fig. 1 an example of the evolution of the mode spectrum is shown. Note the growth of the unstable higher order modes which are nonlinearly excited. These modes will in turn dominate the evolution and it is clear that the asymptotic development would be significantly altered if the system was truncated and these modes not included. For the case of interaction between whistler waves and the slow magnetostatic waves a clear recurrent behaviour was

not observed, and the energy was constantly spreading to the higher mode numbers, which is in agreement with predictions of a qualitative analytical theory. The modulation has a spatial structure resembling cells stretched along the z-axis.

3.3.4 Plasma Transport Due to Electrostatic Turbulence

(Bo Gervang, J.P. Lynov, P. Michelsen, and J. Juul Rasmussen)

The energy confinement of a fusion plasma is limited by the radial heat and particle transport. This transport has long been known to be much larger than the one calculated from the classical theory of diffusion. The so-called anomalous diffusion is believed to be due to electrostatic and magnetostatic fluctuations of micro-instabilities in the plasma driven by density and temperature gradients which cause an enhanced radial plasma transport. Fluid simulations oriented to understand this transport have resulted in transport coefficients in agreement with those found analytically from quasi-linear theory. However, the results can only in some cases describe the experimental results correctly, but cannot at all describe some phenomena such as the transition between the low and high confinement (L- and H-mode).

A theoretical and numerical study was initiated in order to investigate specific physical phenomena of the transport, especially those connected with transport due to coherent structures. This study is concentrated on electrostatic modes in magnetised plasmas, such as drift waves and ηi modes, and also includes the effect of velocity shear which may be important for the transition from L- to H-modes in tokamak plasmas. The numerical methods are based on the highly accurate spectral methods that have been developed in the section mainly for investigations of fluid dynamic systems in which large-scale coherent structures are a typical feature of two-dimensional turbulence. It is not clear whether such structures will exist in more complex models where two or more fields are coupled. However, it has been shown that they may exist in simplified models for the ηi modes. If they also appear under more realistic conditions, they will have strong influence on the modelling of transport. Scaling arguments based on quasi-linear transport coefficients will consequently not be adequate.

3.3.5 Visualisation of Numerical Data

(L. Bækmark, J.P. Lynov, and P. Michelsen)

The visualisation program FRAME described last year was further developed and implemented on the new HP-735 workstation. The purpose of the program, which is based on the UNIRAS graphical system, is to make the data visualisation process easy and flexible for the user. The program is made for visualisation of a time sequence of two-dimensional flow data, but can be used for all kinds of 2D or 3D data sets. A collection of transformation subroutines was developed to provide the possibility of transforming the input data before the visual presentation. The input flow data may be, e.g., Fourier or Chebyshev modes, and can, after the relevant inverse transformation, be presented in configuration space. The screen and hardcopy presentation consist of a number of plots (contour, surface, etc.) each placed in a spreadsheet system of rows and columns. After transformations and processing new data files may be produced: (a) unipict files for further processing and layout adjustments with the UNIEDIT program, (b) targa files for video animation of longtime sequences or for dias production, and (c) HDF-files to be used with the NCSA Ximage/Collage program for direct animation on screen.

Examples of output may be found in other contributions of this report.

3.3.6 A Phase Screen Approach to Coherent Scattering in Fluids

(R.V. Edwards (Case Western Reserve University, Cleveland, Ohio, USA), L. Lading, and V.O. Jensen)

Laser anemometry (velocimetry) based on particle scattering is well established. However, in certain fluids particles cannot be present. This is, e.g., the case in a fusion plasma. In such systems it may be possible to measure transport properties of large-scale fluctuations on the basis of light scattering/diffraction from small-scale structures convected by the larger scales[1]. We have adapted a phase screen approach to the analysis of such systems. A two-point correlation scheme has been devised that allows for a better spatial selectivity than conventional reference beam Doppler systems. The concept is based on a combination of time-of-flight and Doppler systems with reference beam detection. The principle may make it possible to separate different types of waves that generate turbulence.

1) Truck, A. et al. (1992). "ALTAIR": An infrared laser diagnostic on the TORE SUPRA Tokamak", Rev. Sci. Instrum. 63, 3716-3724.

3.3.7 Experimental Investigation of Edge Localised Modes in JET

(A. Lindholm Colton)

Tokamak plasmas are known to exist in two different modes: an *L*-mode with low confinement and an *H*-mode with high confinement. When in an *H*-mode it is known that edge localised modes (ELMs) can occur on the surface of the plasma. These ELMs tend to increase the particle losses from the plasma. In general, ELMs should therefore be avoided, but controlling their appearance might give the possibility of controlling the plasma density.

The aim of the investigation was to examine the nature of ELMs occurring in the JET plasma with the purpose of finding ways to predict and control their appearance. The main findings during the work are:

- The development of temperature and density profiles in an *H*-mode plasma is studied.
- The changes in temperature and density profiles during ELMs are measured.
- The level of fluctuations during ELMs is measured.
- The repetition frequency of the occurrence of ELMs in a newly formed *H*-mode plasma is determined.
- Characteristic orbits in a temperature-density plot during ELMs are found (see Fig. 1)

The main conclusion from the work is that it is very likely that it will be possible to find ways to control and master the occurrence of ELMs in the JET plasma to such a degree that they can be used as a tool for controlling the profile of the plasma density and temperature and thereby keep the plasma in the *H*-mode for a long time. Much more exploratory work has, however, to be carried through to reach that goal.

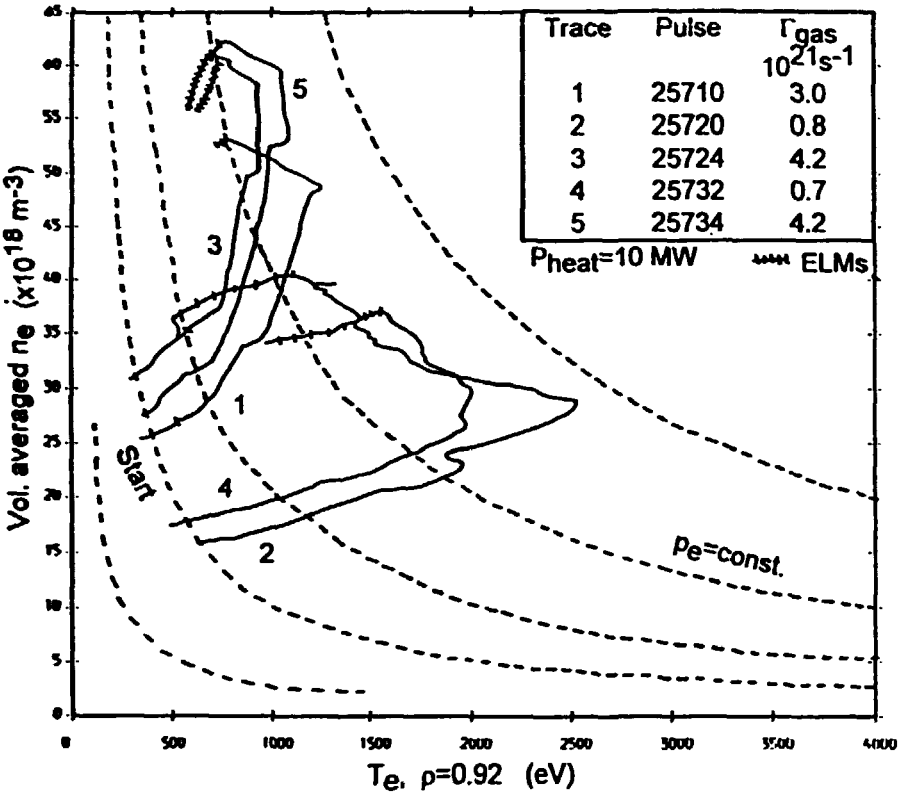

Figure 1. The trajectory in n-T space during the H-mode and the ELMs period afterwards for five discharges with varying gas fuelling rate and similar heating power.

3.3.8 Magnetic Stresses in Ideal MHD Plasmas

(V.O. Jensen)

A comprehensive study of the advantages of using magnetic stresses for determining steady state equilibria of ideal MHD plasmas has been undertaken. The basic equations are:

$$\text{the force density equation,} \quad \mathbf{j} \times \mathbf{B} = \nabla p, \tag{1}$$

$$\text{the Maxwell equations,} \quad \nabla \times \mathbf{B} = \mu \mathbf{j} \quad \text{and} \quad \nabla \cdot \mathbf{B} = 0. \tag{2}$$

Although the magnetic force densities given by the left-hand side term in Eq. (1) are volume forces, it appears that the resulting force on any finite volume element in a plasma can always be calculated by integrating magnetic stresses and particle pressures over the surface of the element. Equilibrium then requires the resulting forces to vanish. Expressions are derived for the various stresses that transmit forces through a surface element, see Fig. 1. Clearly, it is advantageous to choose, whenever possible, volumes with surfaces that are either parallel or perpendicular to the magnetic lines of force. For such surfaces the magnetic stresses are reduced to an isotropic compressive stress, $B^2/2\mu_o$, and a tensile stress, B^2/μ_o, acting parallel to the field lines.

The main purpose of this study is to demonstrate that magnetic stresses offer an alternative and simple method to calculate equilibrium conditions for ideal MHD plasmas. The method has the advantage of offering a simple, physical interpretation of the various terms encountered in the calculations. It also facilitates an assessment of the approximations used in the derivations. Finally, the improved

physical understanding facilitates a quick assessment of the impact on the plasma of imposed changes in the confining field.

In this work conditions for equilibria of axisymmetric toroidal plasmas are reconsidered. It is shown that a purely toroidal magnetic field can prevent a plasma from expanding in the direction of the minor radius only at the expense of an expansion in the direction of the major radius which is twice as fast as it would have been without the toroidal field. The virial theorem is rederived and discussed in terms of the magnetic stresses. Finally, the Grad-Shafranov shift is rederived, and all the terms in the expression for the shift are explained in terms of magnetic stresses.

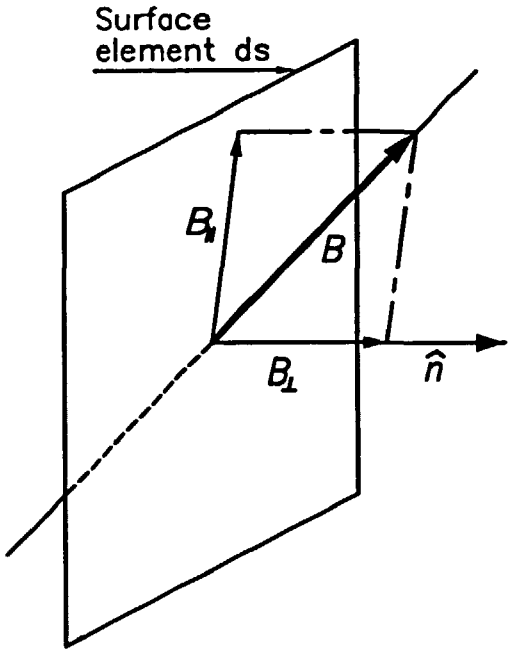

Active stresses

Shear :	$B_\parallel B_\perp/\mu_o$	$[\uparrow(\hat{B}_\perp \times \hat{B}_\parallel) \times \hat{n}]$
Tensile :	$B_\perp^2/\mu_o$	$[\longrightarrow \hat{n}]$
Compressive :	$B^2/2\mu_o$	$[\longleftarrow -\hat{n}]$
Particle pressure :	p	$[\longleftarrow -\hat{n}]$

Figure 1. Active stresses acting on a surface element ds. $\hat{n}$ is a unit vector normal to ds. The forces are transmitted through ds to the volume behind ds. The directions of the various forces are indicated in the brackets with arrows and given in vector expressions.

4 Pellet Injectors for Fusion Experiments

4.1 Introduction

A pellet injector which can inject frozen fuel pellets into fusion plasmas has been developed over the last years. The department has offered to build injectors for fusion laboratories on commercial terms. During 1993 the work has been concentrated on the construction of two systems for the Italien fusion experiments FTU in Frascati and RFX in Padova.

4.1.1 Construction of Multishot Pellet Injectors for FTU, Frascati, and RFX, Padova

(H. Sørensen, A. Michelsen, B. Sass, K-V. Weisberg, and J. Bundgaard* (*Engineering and Computer Department))

The multishot pellet injector systems developed at Risø have the following main characteristics:

- Eight pellets units.
- Pneumatic acceleration, fast valve, high pressure reservoir.
- In situ pellet condensation.
- Velocities ~500 to ~1500 m/s.
- D_2 and H_2 pellets, $5 \cdot 10^{18}$ to $4 \cdot 10^{20}$ atoms/pellet.
- Mass and velocity measured in flight.
- High reproducibility:
  - mass ±10%,
  - velocity ±3%,
  - angle scatter ~ 0.025°.
- Minimum driver gas into the plasma.
- Low liquid He consumption ($\sim 4\ell/h$).

During the period from the spring of 1992 to the end of 1993 a multishot pellet injector for FTU was built, tested, and delivered to Frascati in December 1993.

During the construction improvements were made and various unexpected problems were met and solved:

- A state machine control is installed as an improvement relative to the earlier used automatic operation which was based on a simple PLC.
- The injector system can fire two pellet sizes H_2 and D_2: six pellets with $1 \cdot 10^{20}$ atoms/pellet and two pellets with $2 \cdot 10^{20}$ atoms/pellet. Unexpected problems in obtaining these pellet sizes were solved.
- Finally, the uplining of the gun barrels caused unexpected problems partly due to contamination of pellet gas. Some of the contamination problems were solved by changing operation procedures. An improved alignment system for the barrels was introduced. These problems caused a delay of nearly four months of the acceptance test.

Parallel with the work on the FTU injector nearly all parts for the RFX injector have been procured and the assembling of this injector was started in December 1993. The injector is scheduled to be delivered in Padova in May 1994.

5 Publications and Educational Activities

5.1 Optics

5.1.1 Publications

Andersen, S.A.; Bak, J.; Clausen, S.; Lindvold, L.R., Flue gas particle monitor. (Risø National Laboratory. Department of Combustion Research, Roskilde, 1993). (Energiministeriets Forskningsudvalg for produktion og fordeling af el og varme. Brændsler og forbrændingsteknik) 71 p.

Chartier, J.M.; Darnedde, H.; Frennberg, M.; Henningsen, J.; Karn, U.; Pendrill, L.; Hu, J.P.; Petersen, J.C.; Poulsen, O.; Ramanujam, P.S.; Riehle, F.; Robertsson, L.; Stahlberg, B.; Wahlgren, H., Intercomparison of Northern European I-127(2) stabilized He-Ne lasers at Lambda = 633 nm. Metrologia (1992) v. 29 p. 331-339.

Chong, T.C.; Lu, Y.F. (eds.), (Singapore National University, Singapore, 1993) p. 162-166.

Edwards, R.V., and Jensen, A.S., "Output statistics in sparsely seeded flows", pp. 204- (- in "Selected papers on Laser Doppler velocimetry", R.J. Adrian, editor SPIE Milestone Series, Volume MS 78 (1993)).

Glückstad, J.; Jørgensen, T.M., En optisk neural sløjfe. Det Neurale Netværk i Danmark (1993) (no. 10) p. 7-8.

Glückstad, J.; Compact adaptive multilayer optoelectronic neutral network. Opt. Comput. Proces. (1993) v. 3 (no. 1) p. 95-102.

Hvilsted, S.; Ramanujam, P.S., Nye materialer husker med laserlys. Risønyt (1993) (no. 1) p. 12-13.

Hvilsted, S.; Ramanujam, P.S., Nye materialer husker med laserlys. PC World (1993) (no. 6) p. 36-38.

Hvilsted, S.; Ramanujam, P.S., 60.000 A4-sider på én kvadratcentimeter. Elteknik (1993) v. 10 (no. 6/7) p. 8-9.

Hvilsted, S.; Ramanujam, P.S.; Andruzzi, F., New side-chain liquid crystalline polyester architecture for erasable optical information storage. In: Proceedings of 34th IUPAC congress. Chemistry for 21st century - the central science. 34. IUPAC congress, Beijing (CN), 15-20 August 1993. (Chinese Chemical Society, Beijing, 1993) p. 540.

Hvilsted, S.; Ramanujam, P.S., Nye polymermaterialer til optisk hukommelse. DOPS-Nyt (1993) v. 8 (no. 3) p. 19-20.

Johansen, P.M.; Skov Jensen, A., Dynamics of magnetophotorefractive wave mixing. In: Photorefractive materials. Effects and devices. PRM '93. Technical digest. Topical meeting on photorefractive materials. Effects and devices, Kiev (UA), 11-15 August 1993. (Ukrainian Academy of Sciences, Kiev, 1993) p. 403-406.

Lading, L.; Edwards, R.V., Laser velocimeters: Lower limits to uncertainty. Appl. Opt. (1993) v. 32 p. 3855-3866.

Lading, L., "Analysis of signal-to-noise ratio of the laser Doppler velocimeter", pp. 105- (- in "Selected papers on Laser Doppler velocimetry", R.J. Adrian, editor SPIE Milestone Series, Volume MS 78 (1993)).

Lading, L.; Hurup Hansen, B., A Complementary method for simultaneous measurements of size and velocity. In: Laser techniques and applications in fluid mechanics. 6. International symposium, Lisbon (PT), 20-23 July 1992. Adrian, R.J.; Durao, D.F.G.; Durst, F.; Heiter, M.V.; Maeda, M.; Whitelaw, J.H. (eds.), Springer-Verlag, Berlin, 1993) p. 118-130.

Lading, L.; Lynov, J.P.; Skaarup, B. (eds.), Optics and Fluid Dynamics Department. Annual progress report for 1992. Risø-R-674(EN) (1993) 58 p.

Lindvold, L.R., Commercial applications of diffractive optical elements. DOPS-Nyt (1993) (no. 2) p. 20-24.

Lindvold, L.R.; Ramanujam, P.S., The use of bacteriorhodopsin as a dynamic holographic media. Esprit basic research programme. Project no. 6863, POPAM. (Risø National Laboratory. Optics and Fluid Dynamics Department, Roskilde, 1993) 24 p.

Lindvold, L.R.; Ramanujam, P.S.; Fernquist, T., Holographically recorded transient gratings in retinylidene films. In: Holographic systems, components and applications. 4. International conference on holographic systems, components and applications, Neuchatel (CH), 13-15 September 1993. (Institution of Electrical Engineers, London, 1993) (IEE Conference Publication, 379) p. 76-79.

Martini Jørgensen, T.; Glückstad, J., En optisk neural sløjfe. Kvant (1993) v. 4 (no. 2) p. 20-21.

Martini Jørgensen, T.; Glückstad, J., Nonlinear noise filtering and texture recognition by an optoelectronic neural network that implements a mean field annealing algorithm. In: Proceedings of 1993 international joint conference on neural networks. Vol. 1. IJCNN '93, Nagoya (JP), 25-29 October 1993. (IEEE, Piscataway, NJ, 1993) p. 813-816.

Pedersen, H.C.; Johansen, P.M.B., Polarization and energy transfer dependencies on crystal depth in self-diffraction in BSO. Pure Appl. Opt. (1993) v. 2 p. 659-676.

Petersen, P.M.; Johansen, P.M.B.; Bruun, P.A.; Pedersen, P.J., Higher spatial harmonics in nonlinear photorefractive interference filters. In: 1. International symposium on laser and optoelectronics technology and applications. Proceedings. ISLOE '93, Singapore (SG), 11-13 November 1993.

Ramanujam, P.S.; Hvilsted, S.; Andruzzi, F., Novel biphotonic holographic storage in a side-chain liquid crystalline polyester. Appl. Phys. Lett. (1993) v. 62 p. 1041-1043.

Ramanujam, P.S.; Hvilsted, S.; Andruzzi, F.; Kulinna, C.; Siesler, H.W., Side-chain liquid crystalline polyesters with unusual optical information storage properties. In: Organic thin films for photonic applications. Conference edition. Topical meeting on organic thin films for photonic applications, Toronto (CA), 5-7 October 1993. (Optical Society of America, Washington, DC, 1993) (Technical Digest Series, 17) p. 244-247.

Ramanujam, P.S.; Lindvold, L.R., Dark spatial solitons in bacteriorhodopsin thin films. Appl. Opt. (1993) v. 32 p. 6656-6658.

Skov Jensen, A., Particle image velocimetry: a new computationally efficient method for decoding of PIV images and investigation of hardware realisations. Risø-R-717(EN) (1993) 40 p.

Sloth Christensen, S.; Martini Jørgensen, T., Description of the Herakles system. Version 2.0. Risø-Dok-287 (1993) vp.

Yura, H.T.; Hanson, S.G.; Grum, T.P., Speckle: Statistics and interferometric decorrelation effects in complex ABCD optical systems. J. Opt. Soc. Am. A (1993) v. 10 p. 316-323.

Yura, H.T.; Hanson, S.G., Laser-time-of-flight velocimetry: Analytical solution to the optical system based on ABCD matrices. J. Opt. Soc. Am. A (1993) v. 10 p. 1918-1924.

5.1.2 Unpublished Contributions

Bak, P.E.; Jørgensen, T.M.; Glückstad, J.; Rose, M.; Sørensen, M.P., Optical wavelet transform. Paper P19. In: Danish Physical Society spring meeting. Abstracts. Danish Physical Society spring meeting, Rødby (DK), 16-18 May 1993. (Danish Physical Society. H.C. Ørsted Institute, Copenhagen, 1993) p. 46.

Bak, P.E.; Jørgensen, T.M.; Glückstad, J.; Rose, M.; Sørensen, M.P., Optical wavelet transform. Paper P27. In: Danish Physical Society spring meeting. Abstracts. Danish Physical Society spring meeting, Rødby (DK), 16-18 May 1993. (Danish Physical Society. H.C. Ørsted Institute, Copenhagen, 1993) p. 50.

Dam-Hansen, C.; Johansen, P.M., Photorefractive interference filters. Dansk Optisk Selskabs Årsmøde 1993. DTH, Lyngby (DK), 25 November 1993. Unpublished. Abstract available.

Hanson, S.G., Ocean remote sensing program. NOAA Wave Propagation Laboratory and NOAA Aeronomy Laboratory, Boulder, CO (US), 3 March 1993. Unpublished.

Hanson, S.G., The HH-VV-paradox in radar scattering: Yet another candidate for the anomali. NOAA Wave Propagation Laboratory and NOAA Aeronomy Laboratory. Interactive seminar series, Boulder, CO (US), 16 February 1993. Unpublished. Abstract available.

Hanson, S.G., SCOPE planning. NOAA Wave Propagation Laboratory and NOAA Aeronomy Laboratory, Boulder, CO (US), 3 June 1993. Unpublished.

Hanson, S.G., Multipath scattering of microwave radiation from the ocean surface. NOAA Wave Propagation Laboratory and NOAA Aeronomy Laboratory, Boulder, CO (US), 20 September 1993. Unpublished. Abstract available.

Hanson, S.G.; Hurup Hansen, B., Optical scheme for 2D measurements of vibrations based on a holographic optical element (HOE). Dansk Optisk Selskabs Årsmøde 1993. DTH, Lyngby (DK), 25 November 1993. Unpublished. Abstract available.

Hvilsted, S.; Ramanujam, P.S., Side-chain liquid crystalline polyesters for optical storage. Afdelingen for Faststoffysik, Risø (DK), 24 March 1993. Unpublished.

Hvilsted, S.; Ramanujam, P.S.; Andruzzi, F., Influence of new architecture for side-chain liquid crystalline polyesters on holographic behaviour. In: Molecular engineering of side chain liquid crystalline polymers. European Polymer Federation workshop, Yverdon-les-Bains (CH), 9-11 June 1993. (Ecole Polytechnique Fédérale de Lausanne, Lausanne, 1993) 1 p.

Hvilsted, S.; Ramanujam, P.S., Optisk informationslagring. Polymerteknisk Selskab, København (DK), 26 October 1993. Unpublished.

Johansen, P.M., Analysis of two incoherently written thick holographic grittings. Fysisk Institut, DTH, Lyngby (DK), 18 January 1993. Unpublished.

Johansen, P.M., Analysis of two incoherent written thick holographic gratings. Optikgruppen. Fysisk Institut. DTH, Lyngby (DK), 26 March 1993. Unpublished.

Johansen, P.M., Current aspects of the photorefractive effect. Afdelingen for Optik og Fluid Dynamik, Risø (DK), 22 September 1993. Unpublished.

Johansen, P.M., Current aspects of the photorefractive effect. Afdelingen for Faststoffysik, Risø (DK), 29 September 1993. Unpublished.

Johansen, P.M., Arbejdet med fotobrydende materialer. Besøg af Professorforeningen fra DTH, Risø (DK), 30 September 1993. Unpublished.

Johansen, P.M., Undersøgelser i fotorefraktive materialer. Besøg af Optikgruppen. Fysisk Institut. DTH, Risø (DK), 5 October 1993. Unpublished.

Lading, L., New technology for diagnostics/sensors. Imperial College, London (GB), 2-4 March 1993. Unpublished.

Lading, L., Pushing the limits of statistical uncertainty. Imperial College, London

(GB), 2-4 March 1993. Unpublished.

Lading, L., Laser anemometry I and II. Optical diagnostics for flow processes. Summerschool, Risø (DK), 26 September - 2 October 1993. Unpublished.

Lading, L., Fourier optical model for the laser velocimeter. Optical diagnostics for flow processes. Summerschool, Risø (DK), 26 September - 2 October 1993. Unpublished. pp. 26.

Lading, L., Signal processing for time resolved measurements. Optical diagnostics for flow processes. Summerschool, Risø (DK), 26 September - 2 October 1993. Unpublished. pp. 49.

Lading, L., Statistics of the photodetector signals. Optical diagnostics for flow processes. Summerschool, Risø (DK), 26 September - 2 October 1993. Unpublished. pp. 63.

Lindvold, L., Laseren og dens industrielle anvendelser. Metalskolen i Jørlunde, 14 April 1993. Unpublished.

Lindvold, L., Lasere og Holografi. Fysik- og Kemilærerforeningers besøg på Risø, 30 September 1993. Unpublished.

Lindvold, L., Laseren og dens industrielle anvendelser. Metalskolen i Holstebro, 2 November 1993. Unpublished.

Olsen, T.; Skov Hansen, R.; Johansen, P.M., Rumlig subharmonisk generation i $Bi_{12}SiO_{20}$. Dansk Optisk Selskabs Årsmøde 1993. DTH, Lyngby (DK), 25 November 1993. Unpublished. Abstract available.

Palmer, J.; Hanson, S.G., DELTAk lidar - a new technique for remotely sensing capillary waves. NOAA Wave Propagation Laboratory and NOAA Aeronomy Laboratory, Boulder, CO (US), 10 February 1993. Unpublished.

Pedersen, H.C.; Johansen, P.M., Subharmonic diffraction in photorefractive crystals. Dansk Optisk Selskabs Årsmøde 1993. DTH, Lyngby (DK), 25 November 1993. Unpublished. Abstract available.

Ramanujam, P.S., Nye materialer til optisk hukommelse. OFD-årsmøde, 29 January 1993. Unpublished.

Ramanujam, P.S., New materials for optical storage and processing. Paper N2. In: Danish Physical Society spring meeting. Abstracts. Danish Physical Society spring meeting, Rødby (DK), 16-18 May 1993. (Danish Physical Society. H.C. Ørsted Institute, Copenhagen, 1993) p. 33.

Ramanujam, P.S., Arbejdet med materialer for optisk lagring. Besøg af Professorforeningen fra DTH, Risø (DK), 30 September 1993. Unpublished.

Ramanujam, P.S., Side-chain liquid crystalline polyesters for optical storage. NORDITA, Copenhagen (DK), 31 March 1993. Unpublished.

Ramanujam, P.S., Molecular addressing? Reversible optical storage in side-chain liquid crystalline polyesters. Danish Institute of Fundamental Metrology, Lyngby (DK), 19 April 1993. Unpublished.

Ramanujam, P.S., Optical storage. Danish-Indian Society, Copenhagen (DK), 29 April 1993. Unpublished.

Ramanujam, P.S., Photochemistry of azobenzenes - still an unsolved problem. Dip. di Ingegneria Chimica. University of Pisa, Pisa (IT), 15 June 199?. Unpublished.

Ramanujam, P.S., Optical storage in side-chain liquid crystalline polyester. National Physical Laboratory, New Delhi (IN), 29 June 1993. Unpublished.

Ramanujam, P.S., New materials for optical storage. Indian Institute of Science, Bangalore (IN), 22 July 1993. Unpublished.

Ramanujam, P.S., Materials for optical storage. Indian Telephone Industries, Bangalore (IN), 10 August 1993. Unpublished.

Ramanujam, P.S., Optical storage. Institution of Electronic Engineers, Bangalore (IN), 10 August 1993. Unpublished.

Ramanujam, P.S., Optisk lagring. Roskilde Rotary, Roskilde (DK), 7 December

1993. Unpublished.

Ramanujam, P.S.; Hvilsted, S., Optisk informationslagring. Folkeuniversitetet i Roskilde, Risø (DK), 3 November 1993. Unpublished. Abstract available.

Tillman, J.E.; Hanson, S.G., Humidity measurements usingsemi-conductor laser. University of Washington, Seattle, WA (US), 26 February 1993. Unpublished.

5.2 Continuum Physics

5.2.1 Publications

Bang, O.; Rasmussen, J. Juul; Christiansen, P.L., On localization in the discrete nonlinear Schrödinger equation. Physica D (1993) v. 68 p. 169-173.

Bergeron, K.; Coutsias, E.A.; Lynov, J.P.; Nielsen, A.H., Numerical simulations of self-organization in 2-D circular shear flows. In: Dynamics and geometry of vortical structures. EUROMECH 305. ERCOFTAC workshop, Cortona (IT), 28 June - 2 July 1993. (Universita Degli Studi Di Roma La Sapienza, Rome, 1993) p. 118-119.

Coutsias, E.A.; Lynov, J.P.; Nielsen, A.H.; Nielsen, M.; Rasmussen, J. Juul; Stenum, B., Numerical and experimental investigations of dipole interactions with straight and curved walls in 2D flows. In: Dynamics and geometry of vortical structures. EUROMECH 305. ERCOFTAC workshop, Cortona (IT), 28 June - 2 July 1993. (Universita Degli Studi Di Roma La Sapienza, Rome, 1993) p. 116-117.

Coutsias, E.A.; Lynov, J.P.; Nielsen, A.H.; Nielsen, M.; Rasmussen, J. Juul; Stenum, B., Two dimensional flow simulations. In: Proceedings of the European convex users conference. The metacomputing concept: Supercomputing power without boundaries. ECUC 93, Bilbao (ES), 27-29 October 1993. (Centro Vasco de Supercomputacion, Zamudio, Bizkaia, 1993) 4 p.

Coutsias, E.A.; Lynov, J.P.; Nielsen, A.H.; Nielsen, M.; Rasmussen, J. Juul; Stenum, B., Vortex dipoles colliding with curved walls. In: Future directions of nonlinear dynamics in physical and biological systems. NATO Advanced Study Institute on future directions of nonlinear dynamics in physical and biological systems, Lyngby (DK), 23 July - 1 August 1992. Christiansen, P.L.; Eilbeck, J.C.; Parmentier, R.D. (eds.), (Plenum Press, New York, 1993) (NATO Advanced Science Institutes Series B: Physics, 312) p. 51-54.

Ellegaard, O.; Schou, J.; Sørensen, H.; Pedrys, R.; Warczak, B., Sputtering of solid nitrogen by keV helium ions. Nucl. Instrum. Methods Phys. Res. B (1993) v. 78 p. 192-197.

Hesthaven, J.S.; Lynov, J.P.; Nycander, J., Dynamics of nonstationary dipole vortices. Phys. Fluids A (1993) v. 5 p. 622-629.

Hesthaven, J.S.; Lynov, J.P.; Rasmussen, J. Juul; Sutyrin, G.G., Transport properties of isolated vortices on the beta-plane. In: Dynamics and geometry of vortical structures. EUROMECH 305. ERCOFTAC workshop, Cortona (IT), 28 June - 2 July 1993. (Universita Degli Studi Di Roma La Sapienza, Rome, 1993) p. 120-121.

Hesthaven, J.S.; Lynov, J.P.; Rasmussen, J. Juul; Sutyrin, G.G., Vortex dynamics in 2-dimensional flows. In: Future directions of nonlinear dynamics in physical and biological systems. NATO Advanced Study Institute on future directions of nonlinear dynamics in physical and biological systems, Lyngby (DK), 23 July - 1 August 1992. Christiansen, P.L.; Eilbeck, J.C.; Parmentier, R.D. (eds.), (Plenum Press, New York, 1993) (NATO Advanced Science Institutes Series B: Physics, 312) p. 59-62.

Hesthaven, J.S.; Lynov, J.P.; Rasmussen, J. Juul; Sutyrin, G.G., Generation of

tripolar vortical structures on the beta plane. Phys. Fluids A (1993) v. 5 p. 1674-1678.

Huld, T.; Nielsen, A.H.; Pécseli, H.L.; Rasmussen, J. Juul, Experimental investigations of two-dimensional plasma turbulence. In: Current research on fusion, laboratory and astrophysical plasmas. International workshop on plasma physics, Pichl (AT), 28 February - 2 March 1991. Kuhn, S.; Schöpf, K.; Schrittwieser, R. (eds.), (World Scientific, Singapore, 1993) p. 243-261.

Jensen, V.O., Risø, year 2000, a strategy. In: Physics problems of ITER and DEMO and possible contributions from existing devices and agreed upgrades and programmes. Workshop on physics problems of ITER and DEMO and possible contributions from existing devices and agreed upgrades and programmes, Lisbon (PT), 24-25 July 1993. (Instituto Superior Técnico, Lisbon, 1993) p. 171-180.

Karpman, V.I., Radiation by solitons due to higher-order dispersion. Phys. Rev. E (1993) v. 47, p. 2073-2082.

Lindholm Colton, A., Experimental investigation of edge localised modes in JET. Risø-R-700(EN) (1993) 164 p.

Lynov, J.P.; Rasmussen, J. Juul, Turbulens og selvorganisering i to-dimensionale systemer. KVANT, Fysisk Tidsskrift (1993), v. 4, No. 4, p. 24-28.

Nielsen, A.H., Electrostatic turbulence in strongly magnetized plasmas. Risø-R-659(EN) (1993) 81 p.

Nycander, J., The difference between monopole vortices in planetary flows and laboratory experiments. J. Fluid Mech. (1993), v. 254, p. 561-577.

Nycander, J.; Lynov, J.P.; Rasmussen, J. Juul, Monopolar vortices in etai-modes. Europhys. Lett. (1993) v. 23 p. 249-255.

Lading, L.; Lynov, J.P.; Skaarup, B. (eds.), Optics and Fluid Dynamics Department. Annual progress report for 1992. Risø-R-674(EN) (1993) 58 p.

Stenum, B.; Schou, J.; Sørensen, H.; Gürtler, P., Luminescence from pure and doped solid deuterium irradiated by keV electrons. J. Chem. Phys. (1993) v. 98 p. 126-134.

Sørensen, H.; Sass, B.; Weisberg, K.-V.; Oomens, A.A.M.; Dijk, G. van; Tielemans, A.J.H., A multishot pellet injector for RTP. In: Fusion technology 1992. Vol. 1. 17. Symposium on fusion technology, Rome (IT), 14 - 18 September 1992. Ferro, C.; Gasparotto, M.; Knoepfel, H. (eds.), (Elsevier Science Publishers, Amsterdam, 1993) p. 647-650.

5.2.2 Unpublished Contributions

Coutsias, E.A.; Lynov, J.P.; Nielsen, A.H.; Rasmussen, J. Juul; Stenum, B., Experimental investigations of dipole interactions with straight and curved walls in 2-D flows. In: Interaction between vorticity fields and boundaries. Book of abstracts. EUROMECH colloquium 300, Istanbul (TR), 27-30 September 1993. Kaykayoglu, C.R.; Graham, J.M.R. (eds.), (European Mechanics Council, Istanbul, 1993) p. 23.

Coutsias, E.A.; Lynov, J.P.; Nielsen, A.H.; Rasmussen, J. Juul; Stenum, B., Numerical investigations of dipole interactions with straight and curved walls in 2-D flows. In: Interaction between vorticity fields and boundaries. Book of abstracts. EUROMECH colloquium 300, Istanbul (TR), 27-30 September 1993. Kaykayoglu, C.R.; Graham, J.M.R. (eds.), (European Mechanics Council, Istanbul, 1993) p. 24.

Hesthaven, J.S., Transport properties of isotropic and anisotropic flows illustrated by particle dynamics. Paper P24. In: Danish Physical Society spring meeting. Abstracts. Danish Physical Society spring meeting, Rødby (DK), 16-18

May 1993. (Danish Physical Society. H.C. Ørsted Institute, Copenhagen, 1993) p. 48.

Jensen, V.O., Plasmafysik 2. Forelæsningsserie. Danmarks Tekniske Højskole, Lyngby (DK), February - June 1993. Unpublished.

Jensen, V.O., Drømmen om en ubegrænset energi. Danmarks Radio TV, Copenhagen (DK), 4 April 1993. Unpublished.

Jensen, V.O., Status of the European fusion programme: JET, ITER. Paper D4. In: Danish Physical Society spring meeting. Abstracts. Danish Physical Society spring meeting, Rødby (DK), 16-18 May 1993. (Danish Physical Society. H.C. Ørsted Institute, Copenhagen, 1993) p. 17.

Jensen, V.O., Compressive and tensile stresses in magnetic fields used as a basis for calculations of plasma equilibria. Paper P25. In: Danish Physical Society spring meeting. Abstracts. Danish Physical Society spring meeting, Rødby (DK), 16-18 May 1993. (Danish Physical Society. H.C. Ørsted Institute, Copenhagen, 1993) p. 49.

Jensen, V.O., Fusionsforskningen har passeret en milepæl. Elsam, Fredericia (DK), 6 May 1993. Unpublished. Abstract available.

Jensen, V.O., Fusionsinterview i serien "Strejftog i Universet", Danmarks Radio, TV, Copenhagen (DK), 20 September 1993. Unpublished.

Jensen, V.O., Fusionsplasmafysik. Forelæsningsserie. Danmarks Tekniske Højskole, Lyngby (DK), September - December 1993. Unpublished.

Lynov, J.P., Coherent structures in two-dimensional flows. Paper M2. In: Danish Physical Society spring meeting. Abstracts. Danish Physical Society spring meeting, Rødby (DK), 16-18 May 1993. (Danish Physical Society. H.C. Ørsted Institute, Copenhagen, 1993) p. 31.

Michelsen, P.; Karpman, V.I.; Lynov, J.P.; Rasmussen, J. Juul, Modulational instability due to nonlinear coupling between high- and low-frequency waves. 5. European fusion theory conference, Madrid (ES), 22-24 September 1993. Unpublished. Abstract available.

Nielsen, A.H.; Bergeron, K.; Coutsias, E.A.; Lynov, J.P., Numerical simulations of self-organization in 2-d circular shear flows. Paper P23. In: Danish Physical Society spring meeting. Abstracts. Danish Physical Society spring meeting, Rødby (DK), 16-18 May 1993. (Danish Physical Society. H.C. Ørsted Institute, Copenhagen, 1993) p. 48.

Rasmussen, J. Juul, Vortex dynamics in two-dimensional flows. 28. Nordic plasma and gas discharge symposium, Wadahl (NO), 8-10 February 1992. Unpublished.

Rasmussen, J. Juul, Vortex dynamics in fluids and plasmas. Physikalisches Kolloquium. Universität Kiel, Kiel (DE), 22 June 1993. Unpublished.

Rasmussen, J. Juul, Two dimensional plasma turbulence. Institut für Experimentalphysik. Universität Kiel, Kiel (DE), 23 June 1993. Unpublished.

Rasmussen, J. Juul, Kohærente strukturer i kontinuumsystemer. Institutkollokvium. Fysisk Institut. Odense Universitet, Odense (DK), 12 October 1993. Unpublished. Abstract available.

Rasmussen, J. Juul, Electrostatic waves and instability in homogeneous, magnetized plasmas. (5 Lectures). Advanced school on waves and instabilities in plasmas. International Centre for Mechanical Sciences, Udine (IT), 20-24 September 1993. Unpublished.

Rasmussen, J. Juul; Stenum, B., Visualization of coherent structures. Optical diagnostics for flow processes. Summerschool, Risø (DK), 26 September - 2 October 1993. Unpublished.

Rasmussen, J. Juul; Stenum, B., Vortices and self-organization in two-dimensional flows. Department of Technical Physics. University of Eindhoven, Eindhoven (NL), 7 December 1993. Unpublished.

Rasmussen, J. Juul; Stenum, B., Eksperimentelle undersøgelser af hvirvelstruktur i væsker. Folkeuniversitetet i Roskilde, Risø (DK), 1 December 1993. Unpublished. Abstract available.

Stenum, B., Experimental investigations of coherent structures. Paper P22. In: Danish Physical Society spring meeting. Abstracts. Danish Physical Society spring meeting, Rødby (DK), 16-18 May 1993. (Danish Physical Society. H.C. Ørsted Institute, Copenhagen, 1993) p. 47.

6 Personnel

Scientific Staff

Christensen, Steen Sloth
Gervang, Bo (from 1 October)
Grimley, Hugh (from 25 January)
Hanson, Steen Grüner
Jensen, Arne Skov
Jensen, Vagn O.
Johansen, Per Michael
Jørgensen, Thomas Martini
Lading, Lars
Lindvold, Lars R.
Lynov, Jens-Peter
Michelsen, Poul
Nielsen, Anders H.
Ramanujam, P.S.
Rasmussen, Jens Juul
Stenum, Bjarne
Sørensen, Hans
Weisberg, Knud-V.

Ph.D. Students

Andersen, Annette (until 31 July)
Dam-Hansen, Carsten (from 1 March)
Hesthaven, Jan S.
Kristensen, Jesper Glückstad
Pedersen, Henrik (from 1 March)

Technical Staff

Bækmark, Lars
Eilertsen, Erik
Hansen, Bengt Hurup
Ibsen, Hjarne Sonne (15 February - 14 September)
Michelsen, Agnete
Moustgaard, Stig (from 26 July)
Nielsen, Henrik Olskjær (until 21 June)
Nielsen, Mogens O.
Rasmussen, Erling

Reher, Børge
Sass, Bjarne
Søefeldt, Allan (from 26 July)
Stubager, Jørgen (from 9 August)
Thorsen, Jess

Secretaries
Astradsson, Lone
Jensen, Elin (from 15 December)
Skaarup, Bitten
Toubro, Lene

Guest Scientist

Bergeron, K., University of New Mexico, USA
Edwards, R.V., Case Western Reserve University, Cleveland, USA
Imam, H., King's College, London, UK
Karpmann, V.I., Racah Institute of Physics, Jerusalem, Israel
Kuznetsov, E.A., Landau Institute for Theoretical Physics, Moscow, Russia
Pécseli, H.L., University of Oslo, Norway
Snezhkin, E.N., Russian Research Center Kurchatov Institute, Moscow, Russia
Sutyrin, G., Institute of Oceanology, Moscow, Russia
Yushina, I., Institute of Oceanology, Moscow, Russia

Short-Time Visitors

Buchhave, P., Technical University of Denmark
Coutsias, E.A., University of New Mexico, USA
Decker, NASA-Lewis Research Center, Cleveland, Ohio, USA
Fraser, S.M., University of Strathclyde, Glasgow, UK
Greenhalgh, D., Cranfield Institute of Technology, Cranfield, UK
Grésillon, D., Laboratoire de Physique des Milieux Ionisés du CNRS, Ecole Polytechnique, Palaiseau, France
Hinsch, K., Carl von Ossietzky Universität, Oldenburg, Germany
Jones, J., Heriot-Watt University, Edinburgh, UK
Keane, R.D., University of Illinois at Urbana-Champaign, Urbana, Illinois, USA
Larsen, P. Scheel, Technical University of Denmark
Nycander, J., University of Uppsala, Sweden
Reitblat, G., Institute of Cybernetic Problems of Russian Academy of Science, Moscow, Russia
Sturman, B.I., Institute of Automation and Electrometry, Novosibirsk, Russia
Turitsyn, S.K., Institute of Automation and Electrometry, Novosibirsk, Russia
Volkov, V., Institute of Cybernetic Problems of Russian Academy of Science, Moscow, Russia
Wigley, G., AVL List GmbH, Graz, Austria

Student Assistants

Poul Erik Bak (1 October - 30 November)
Schmidt, Michel (18-29 January, 9 August - 17 September, 16-23 December)

Bibliographic Data Sheet **Risø-R-715(EN)**

Title and author(s)

Optics and Fluid Dynamics Department
Annual Progress Report for 1993

S.G. Hanson, L. Lading, P. Michelsen, and B. Skaarup

ISBN	ISSN
87-550-1937-4	0106-2840 0906-1797

Dept. or group	Date
Optics and Fluid Dynamics Department	January 1994

Groups own reg. number(s)	Project/contract No.

Pages	Tables	Illustrations	References
58		27	24

Abstract (Max. 2000 char.)

Research in the Optics and Fluid Dynamics Department is performed within the following two programme areas: optics and continuum physics. In optics the activities are within (a) optical materials, (b) quasi-elastic light scattering and diagnostics in solids, fluids, and plasmas, and (c) optical and electronic information processing. Within continuum physics the activities are within (a) studies of nonlinear dynamical processes in continuum systems, (b) investigations of problems with relevance to fusion plasma physics. The injection of pellets in fusion experiments has been investigated and pellet injectors to European fusion experiments are manufactured. The department is also responsible for the EURATOM collaboration within fusion plasma physics. A summary of activities in 1993 is presented.

Descriptors INIS/EDB

DYNAMICS; FLUIDS; LASERS; NONLINEAR OPTICS; NONLINEAR PROBLEMS; NUMERICAL SOLUTION; PLASMA; PROGRESS REPORT; RESEARCH PROGRAMS; RISOE NATIONAL LABORATORY; THERMONUCLEAR REACTIONS

Available on request from:
Risø Library, Risø National Laboratory (Risø Bibliotek, Forskningscenter Risø)
P.O. Box 49, DK-4000 Roskilde, Denmark
Phone (+45) 46 77 46 77, ext. 4004/4005 · Telex 43 116 · Fax (+45) 46 75 56 27

RISØ

OBJECTIVE

The objective of Risø National Laboratory is to further technological development in three main areas: energy, environment and materials.

USERS

Risø's scientific results are widely applied in industry, agriculture and public services. Risø contributes its share of new knowledge to the global research community.

RESEARCH PROFILE

Risø emphasises long-term and strategic research providing a solid scientific foundation for the technological development of society.

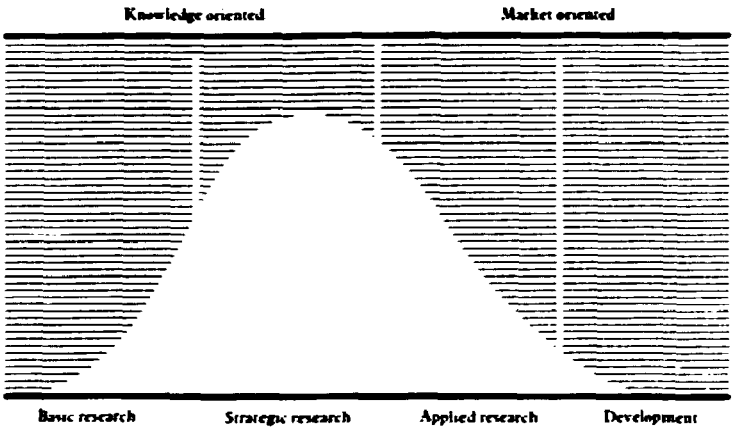

PRIORITY AREAS

- **Combustion and gasification**
- **Wind energy**
- **Energy materials**
- **Energy and environmental planning**
- **Assessment of environmental loads**
- **Reduction of environmental loads**
- **Safety and reliability of technical systems**
- **Nuclear safety**
- **Atomic structure and properties of materials**
- **Advanced materials and materials technologies**
- **Optics and fluid dynamics**

Risø-R-715(EN)
ISBN 87-550-1937-4
ISSN 0106-2840
ISSN 0906-1797

Available on request from:
***Risø* Library**
***Risø* National Laboratory**
P.O. Box 49, DK-4000 Roskilde, Denmark
Phone +45 46 77 46 77, ext. 4004/4005
Telex 43116, Telefax 46 75 56 27